Modeling a Standing Wave Linear Accelerator's Dispersion Relationship and Field Profile via an Equivalent Circuit and Numerical Analysis.

Stephen James Vanderet

Submitted to the faculty of the University Graduate School
in partial fulfillment of the requirement
for the degree of
Master of Science
Department of Physics,
Indiana University
October 2011

ProQuest LLC.
789 East Eisenhower Parkway
P.O. Box 1346
Ann Arbor, MI 48106 - 1346

Accepted by the Graduate Faculty, Indiana University, in partial fulfillment of the requirements for the degree of Masters of Science.

Master's Thesis Committee

Shyh-Yuan Lee, PH.D
Committee chair

Paul E. Sokol, PH.D
Committee member

Rex Tayloe, PH.D
Committee member

David H. Whittum, PH.D, P.E.
Committee member & adviser

Acknowledgment

First and foremost, I would like to acknowledge and thank David Whittum for the time he spent fulfilling the role of an advisor and mentor over the course of this five year program. Without his insight and teaching this thesis would not have been possible. Also, thank you Arthur Salop at Varian Medical Systems for your help in verifying the numerical calculations. Thanks to Varian Medical Systems in general and specifically Mark Trail for allowing me to complete this masters program as part of my training. I am grateful for the thesis committee member's time and consideration. Also, a special thanks to Susan Winchester, Tracy McGooky, and Erin Beth Arthur for their assistance in navigating the required bureaucracy. Thanks to the DOE, Indiana University Physics Department, and all the teachers that make the IU/USPAS's masters program possible.

Stephen Vanderet

Modeling a Standing Wave Linear Accelerator's Dispersion Relationship and Field Profile via an Equivalent Circuit and Numerical Analysis.

Industrial and medical standing wave linear accelerators are used to create mega voltage x-rays, which in turn are used to for imaging and oncology. In both fields, biperiodic structures operating in the $\pi/2$ mode dominate the field. Cavity tuning errors in these structures can produce unacceptable variations from the designed peak electric field values. Dispersion equations derived from equivalent circuit models have historically been used to calculate the stopband in inductively coupled structures. This thesis reviews two of those approaches, and in addition derives a new dispersion relationship for a capacitively coupled structure. This biperiodic capacitively coupled dispersion equation is shown to provide excellent agreement with a brazed, 9 mode, biperiodic, capacitively coupled x-band structure. An equivalent circuit model is then solved numerically to illustrate the effect of tuning errors on a biperiodic 23 cavity capacitively coupled x-band standing wave accelerator's electric field profile. Plots of field profiles caused by known tuning errors are provided. These can be used to diagnose the cause of unexpected field slope and/or steps.

Table of Contents

1 Introduction

Standing wave linear accelerators are structures composed of coupled cavities. When microwave power is feed into a standing wave accelerator, electromagnetic fields form and oscillate in the structure's cavities. Since all the cavities are coupled, the structure behaves like a series of coupled oscillators. Ideally the individual cavities are "tuned" such that a specific normal mode, conducive to particle acceleration, is formed when the structure is driven at the operating frequency. It is desirable to understand how these normal modes depend on the individual cavities resonant frequencies, so that accelerating structures can be manufactured in a reliable and repeatable process.

In order to study this dependence, an equivalent circuit model is employed. In general, the model is a series of coupled RLC tank circuits; where the resistor relates to the resistance experienced by a cavity's surface current, the inductor relates to a cavity's ability to store magnetic energy, the capacitor relates a cavity's ability to store electrical energy, and the mutual inductance and or mutual capacitance relates inter-cavity coupling. Such models are used as both quantitative tools to "tune" accelerators, and as qualitative tools to diagnose a structure's non ideal normal mode behavior.

It is worth noting that an equivalent circuit model is not the only option for modeling a standing wave accelerator's normal modes. Modern 3D electromagnetic software such as CST Microwave Studio would make the equivalent circuit model obsolete if computer power were unlimited. These programs can do everything an equivalent circuit model

can, and many things an equivalent circuit model can not. However, the trade off is that these codes are much more computationally intensive than a code which makes use of an equivalent circuit model. This makes 3D electromagnetic codes excellent for modeling segments of an accelerator, but limits their utility for modeling an entire coupled cavity accelerator.

2 Background

2.1 Single Cavity modes

Any volume enclosed by an electric conductor will have an infinite number of electromagnetic resonant modes associated with its given dimensions. An analytic solution for the field distribution and frequency of these modes exists for simple geometries such as the cylindrical pill box. [Jac 62]

$$f_{mnp}^{TM} = \frac{c}{2\pi\sqrt{\mu\varepsilon}}\sqrt{\left(\frac{\chi_{mn}}{a}\right)^2 + \left(\frac{p\pi}{l}\right)^2} \tag{2.1}$$

Where a is the radius of the pill-box, l is the cavities length, and χ is the n^{th} zero of an m^{th} order Bessel's function, c is the speed of light in vacuum, μ & ε are properties of the material in the volume, and m, n, and p are mode numbers with the following ranges $0 \le m < \infty$, $1 \le n < \infty$, and $0 \le p < \infty$. Equations (2.1), (2.3), and (2.4) assume that the walls of the cavity are infinitely conductive and that the cavity is filled uniformly with lossless dielectric. An equation for the TE modes is not shown because of these infinite modes most linear accelerator cavities employ only a TM_{010} like mode or *fundamental mode*.

$$f_{010}^{TM} = \frac{c}{2\pi\sqrt{\mu\varepsilon}}\frac{2.405}{a} \tag{2.2}$$

There are practical reasons for this. This mode allows beam holes to go in center of the cavity (along the z-axis) where the E-field is peaked and the B-field is zero, allowing the beam of charged particles to be accelerated by the electric field and not be deflected by the magnetic field. The explicit solutions for the TM_{010} electric and magnetic fields are shown (2.3)(2.4).

$$E_z = E_0 J_0\left(\frac{2.405\left(\sqrt{x^2+y^2}\right)}{a}\right)e^{-i\omega t} \tag{2.3}$$

$$H_\phi = -j\sqrt{\frac{\varepsilon}{\mu}}E_0 J_1\left(\frac{2.405\left(\sqrt{x^2+y^2}\right)}{a}\right)e^{-i\omega t} \tag{2.4}$$

Both the electric and magnetic field exist in each cavity at the same time. The magnetic field is created by the time dependent electric field and the electric field is in turn created by the time dependent magnetic field which causes these fields to be 90˚ out of phase and the magnitude of each field to oscillate harmonically at the resonant frequency.

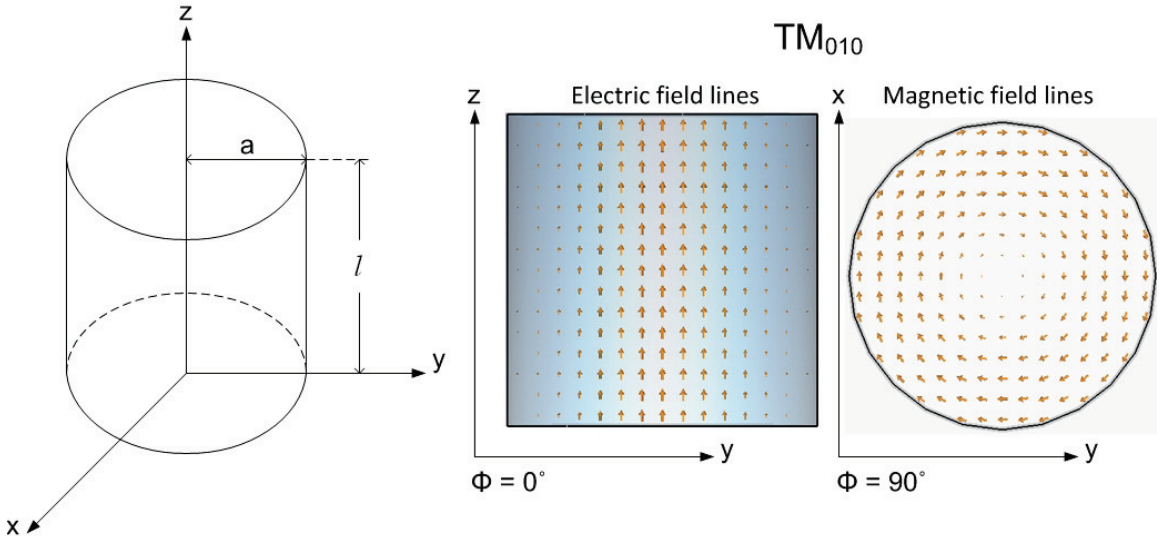

Figure 2-1: TM_{010} field lines inside an ideal pillbox.

In practice electromagnetic modeling software is used to calculate cavity fields and resonant modes. However, this analytic solution is still useful to check the accuracy of new electromagnetic codes, or to provide a rough scaling for a new cavity design.

2.2 Coupled Cavity Normal Modes

RF cavities can be coupled together in two ways. They can be coupled inductively and/or they can be coupled capacitively. When they are coupled inductively some of the magnetic energy propagates from one cavity to the other, and when they are coupled capacitively, some of the electric energy propagates from one cavity to the other.

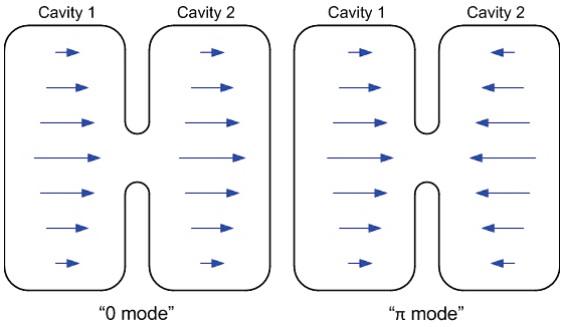

Figure 2-2: Electric field lines of the TM_{010} mode shown in blue for periodic, on axis, capacitively coupled pillboxes.

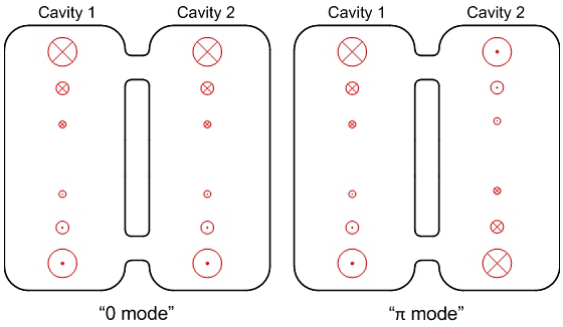

Figure 2-3: Magnetic field lines of the TM_{010} mode shown in red for periodic, on axis, inductively coupled pillboxes.

Figs. (2-2) and (2-3) illustrate that the physical location of coupling slots determines how a structure is coupled. Notice that two normal modes are shown in Figs. (2-2) and (2-3). When *N* cavities are coupled together in a standing wave structure, each TM and TE single cavity mode is split up in *N* normal modes corresponding to different electromagnetic phase advance from cavity to cavity [Wan 98]. The normal modes are named by their phase advance in radians. The 0-mode has no phase advance from cavity to cavity, hence the "0", since neighboring cavities are 0 radians out of phase with respect to each other. In the π-mode neighboring cavities are 180° or π radians out of phase.

With standing wave boundary value conditions, it is known that the extremum frequency normal modes will always be the 0-mode and π-mode. Also, the modes in-between them

(with respect to frequency) will always differ in phase by $\pi/(N-1)$ radians. This rigid allowable phase advance between modes is a result of other phase advance values between cavities being canceled out by reflections.

Note that, the word mode is being used twice to describe related but different types of resonance. Within the context of standing wave accelerators it's common to only refer to the normal modes without reference to TM and TE single cavity modes, since it's usually obvious the TM_{010} like mode is the one being employed.

For example Fig. (2-4) shows a structure with 3 cavities. This structure has an infinite number of 0-modes corresponding to the 0-mode of each TM and TE single cavity mode. However, the 0-mode of the TM_{010} like mode is often referred as if it were the only 0-mode, since it's often the only one that matters. To help alleviate this confusion, I'll use the term "single cavity modes" to describe the TM and TE modes described in section 1.2 and the term "normal modes", or just modes, to describe a resonances associated with coupled cavities.

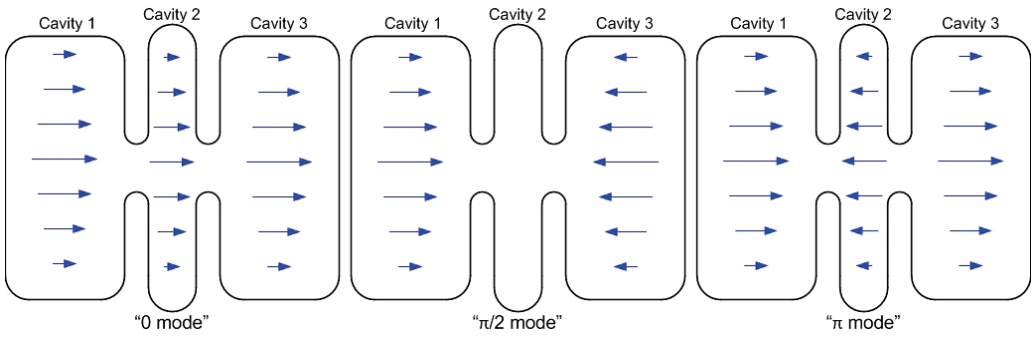

Figure 2-4: Electric field lines of the TM_{010} single cavity mode shown in blue for a 3 cavity segment of a biperiodic on axis capacitively coupled pillboxes. All three of this structure's normal modes are shown.

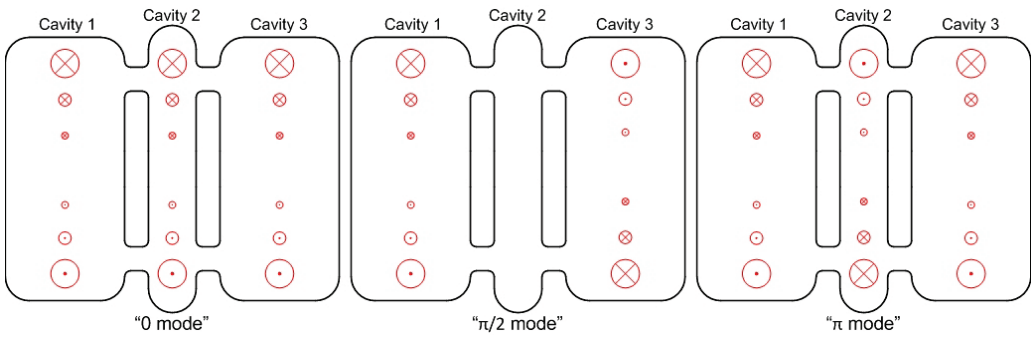

Figure 2-5: Magnetic field lines of the TM_{010} mode shown in red for a 3 cavity segment of a biperiodic on axis capacitively coupled pillboxes. All three of this structure's normal modes are shown.

For cavities to couple, their single cavity modes need to be similar frequencies. However, there is no requirement on the specific shape of the cavities. This give rise to different possible accelerator designs. Biperiodic structures usually consist of a high quality factor (Q) accelerating cavity (a-cell) and a relatively low Q coupling cavity (c-cell). Guides operating in the π/2 mode have minimal field in the c-cells, which causes losses in these cavities to be low despite their having a relatively small quality factor [Wan 98]. Biperiodic structures are the standard when it comes to medical and industrial accelerators. However, other designs are possible. For example, back in 1975, a tri-periodic standing wave accelerator operating in the $2\pi/3$ mode was considered [Sch 75], and periodic structures are commonly used in super conducting accelerators.

2.3 The Tank Circuit

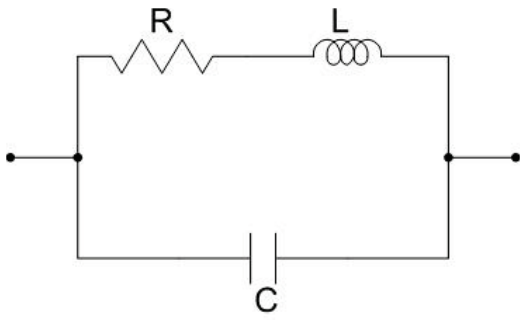

Figure 2-6: The tank circuit is the basic building block of the standing wave linear accelerator circuit equivalent model used in this paper.

This circuit goes by a few names: the antiresonant circuit, the tank circuit, and the electrical resonator circuit. I prefer tank circuit. At resonance, the capacitor and the inductor trade the same stored energy on alternate half cycles. When the capacitor discharges, the inductor charges, and vice versa. This makes the circuit ideal for modeling resonant cavities which analogously trade energy between oscillating electric and magnetic fields. These fields oscillating in resonant cavities induce and are driven by surface currents in the cavity's walls. These surface currents experience ohmic losses analogous to the ohmic losses in the tanks circuit's resistor.

In order to compare a resonant cavity to a tank circuit the resonant frequency and the quality factor are used. Both of these attributes have the similar meaning in the tank circuit and the resonant cavity, despite being governed by different mechanisms. In the tank circuit the resonant frequency is the frequency at which the impedance becomes purely resistive via the capacitive reactance canceling with the inductive reactance.

$$\omega_0 = 2\pi f = \sqrt{\frac{1}{LC} - \frac{R^2}{L^2}} \approx \frac{1}{\sqrt{LC}} \text{ when } \left[R << \omega_0 L\right] \tag{2.5}$$

Accelerator cavities are made out of pure copper and are operated at microwave frequencies, so the approximation is reasonable. The quality factor in the tank circuit is a dimensionless ratio that compares the reactive energy stored in the inductor or the capacitor each cycle to the resistive energy dissipated.

$$Q = 2\pi\left(\frac{\text{maximum energy stored per cycle}}{\text{energy dissipted per cycle}}\right) \tag{2.6}$$

$$Q = \frac{1}{\omega_0 CR} = \frac{\omega_0 L}{R} \tag{2.7}$$

These two relationships will be used later to transform a series of coupled tank circuits into a model of a chain of coupled resonant cavities.

3 Dispersion Equations

The dispersion relationship of a standing wave accelerator gives the frequency of the structure's normal modes; typically as a function of phase advance, cavity tune, and coupling strength. One way to derive an approximation of this relationship is to use an equivalent circuit model. A group at Los Alamos did this in the mid 60's [Nag 67] with great success. The first two sections of this chapter are a review of their work on inductively coupled periodic and biperiodic standing wave structures. The third and fourth sections look at how both the periodic and biperiodic dispersion relationships are affected by shifting from inductive coupling to capacitive coupling.

Some simplifications to the circuit equivalent model are required in order to get analytic solutions. First, all cavities will be considered lossless. Resistance will be included at the beginning of each derivation, because it will be useful later when these same problems are solved with numerical techniques. Second, we will be satisfied to merely solve the homogeneous solution to the equivalent circuit model, as that is enough to find excellent agreement with experimental data for guides operating in steady state [Kap 68].

The dispersion relation will illustrate terms such as bandwidth and stopband. In addition, it will shed some light on what is meant when a biperiodic structure is said to be "tuned." These concepts are required to understand the cause and effect of tuning errors associated with biperiodic standing wave accelerators.

3.1 Inductively Coupled Periodic Standing Wave Structure

The circuit equivalent model for this structure consists of N identical tank circuits coupled together via mutual inductance. For the periodic structure, only nearest neighbor coupling will be considered. This means mutual inductance will only exist between adjacent cavities as shown in Figs. (3-1) and (3-2).

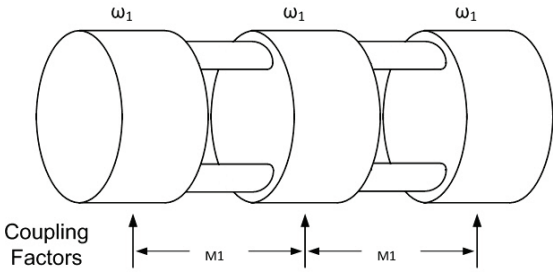

Figure 3-1: Periodic, inductively coupled standing wave structure.

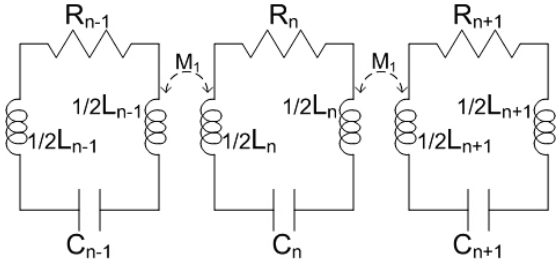

Figure 3-2: Equivalent circuit model of Fig (3-1).

Using Kirchhoff's loop in the n[th] tank circuit yields the following relationship.

$$0 = i_n R_n + \frac{\int_0^t i_n(\tau)\,d\tau}{C_n} + L_n \frac{di_n}{dt} + M_1 L_n \frac{di_{n-1}}{dt} + M_1 L_n \frac{di_{n+1}}{dt} \tag{3.1}$$

M_1 is a unitless coupling constant which is defined such that the quantity $M_1 L_n \frac{di_{n-1}}{dt}$ is the voltage created across $L_n = 1/2\,L_n + 1/2\,L_n = L_{eff}$ when the current in cell $n-1$ changes with respect to time. Since each cavity is identical in this model, the coupling between adjacent cavities is the same. The Laplace transform Eqs (3.2) and (3.3) are used to greatly simplify the problem.

$$\mathcal{L}\left\{\int_0^t f(\tau)\,d\tau\right\} = \frac{1}{s}\mathcal{L}\{f(t)\} = \frac{f(s)}{s} \tag{3.2}$$

$$\mathcal{L}\{f'(t)\} = s\mathcal{L}\{f(t)\} - f(0) = s \cdot f(s) - f(0) \tag{3.3}$$

Now with the assumption that all currents equal zero at time zero (3.1) simplifies to (3.4).

$$0 = i_n\left(R_n + \frac{1}{sC_n} + sL_n\right) + i_{n-1}sM_1L_n + i_{n+1}sM_1L_n \tag{3.4}$$

Because the steady state solution is what is of interest, the following substitution is made $s = j\omega$.

$$0 = i_n\left(R_n + \frac{1}{j\omega C_n} + j\omega L_n\right) + i_{n-1}M_1 j\omega L_n + i_{n+1}M_1 j\omega L_n \tag{3.5}$$

Next, (3.5) is divided by $jL_n\omega$ and we introduce a constant k_1 such that, $M_1 = k_1/2$. This may seem arbitrary since they are both just coupling constants, however this coupling constant k is what is used in the Los Alamos papers. So in order to get the same results that substation is required. The factor of 2 differences between the two coupling terms comes from the fact that I made my equivalent circuit model with half the inductance of their model.

$$0 = i_n\left(1 + \frac{R_n}{\omega jL_n} - \frac{1}{\omega^2 L_n C_n}\right) + \frac{k_1}{2}\left(i_{n-1} + i_{n+1}\right) \tag{3.6}$$

Using equations (2.5) and (2.7) equation (3.6) is transformed from an equation describing a series of coupled tank circuits into one describing of a chain of inductively coupled resonant cavities.

$$0 = i_n\left(1 + \frac{\omega_n}{\omega jQ_n} - \frac{\omega_n^2}{\omega^2}\right) + \frac{k_1}{2}\left(i_{n-1} + i_{n+1}\right) \tag{3.7}$$

In order to simplify the problem the cavities are assumed to be lossless, which corresponds to an infinite *Q*. Since all the cavities are identical let $\omega_n = \omega_0$

$$0 = i_n\left(1 - \frac{\omega_0^2}{\omega^2}\right) + \frac{k_1}{2}\left(i_{n-1} + i_{n+1}\right) \tag{3.8}$$

At this point we assume the correct solution for the current in the n^{th} cavity.

$$i_n(q) = A\cos\left(\frac{\pi qn}{N-1}\right)e^{j\omega_q t} \tag{3.9}$$

Where N is the number of cells in the structure, q is the mode number and has a range of $0 \geq q \leq (N-1)$, and n is the cavity number with a range of $1 \geq n \leq N$.

Motivation for choosing this solution

- Since the cavities are lossless and identical, the peak current in each cavity must be equal to some constant $[A]$
- Each cavity will oscillate harmonically at its normal mode frequency $\left[e^{j\omega_q t}\right]$
- Since this is a standing wave structure, phase advance from one mode to the next will be given by $\frac{\pi}{(N-1)}$, and cavity to cavity phase advance of any given mode will be given by $\frac{\pi qn}{N-1}$. So the magnitude of the current in cell n will be affected by the term $\left[\cos\left(\frac{\pi qn}{N-1}\right)\right]$

Substituting (3.9) into (3.8) and dividing out the exponential factor and the constant A yields.

$$0 = \left(1-\frac{\omega_0^2}{\omega^2}\right)\cos\left(\frac{\pi qn}{N-1}\right) + \frac{k_1}{2}\left(\cos\left(\frac{\pi q}{N-1}(n-1)\right) + \cos\left(\frac{\pi q}{N-1}(n+1)\right)\right) \tag{3.10}$$

Let $a = \frac{\pi qn}{N-1}$, $b = \frac{\pi q}{N-1}$ in order make use of (3.12).

$$0 = \left(1-\frac{\omega_0^2}{\omega^2}\right)\cos(a) + \frac{k_1}{2}\left[\cos(a-b) + \cos(a+b)\right] \tag{3.11}$$

$$\cos(a+b) + \cos(a-b) = 2\cos(a)\cos(b) \tag{3.12}$$

$$\omega^2 = \frac{\omega_0^2}{1 + k_1 \cos\left(\frac{\pi q}{N-1}\right)} \tag{3.13}$$

Equation (3.13) is the dispersion relationship for an inductively coupled, periodic, lossless, standing wave chain of resonant cavities. From (3.13), it's apparent that highest mode number (N-1) will have a resonant frequency equal to $\omega_0 / \sqrt{1-k}$, where ω_0 equals to the resonant frequency a single cavity would resonate at if it were isolated from the rest of the chain. Similarly, from (3.13) it's apparent that the lowest mode number (0) will have a resonant frequency equal to $\omega_0 / \sqrt{1+k}$. The bandwidth of the structure is equal to (3.14)

$$BW = \omega_0 \left(\frac{1}{\sqrt{1-k}} - \frac{1}{\sqrt{1+k}} \right) \tag{3.14}$$

The bandwidth of a linear accelerator is an important design parameter. Guides with larger bandwidth have larger mode separation, which is generally considered desirable in accelerators. However, as the bandwidth is increased the coupling factor becomes more significant in determining the structures resonance frequencies. Form (3.14), it's apparent that BW approaches 0 as the coupling approaches 0, and increases as the coupling increases.

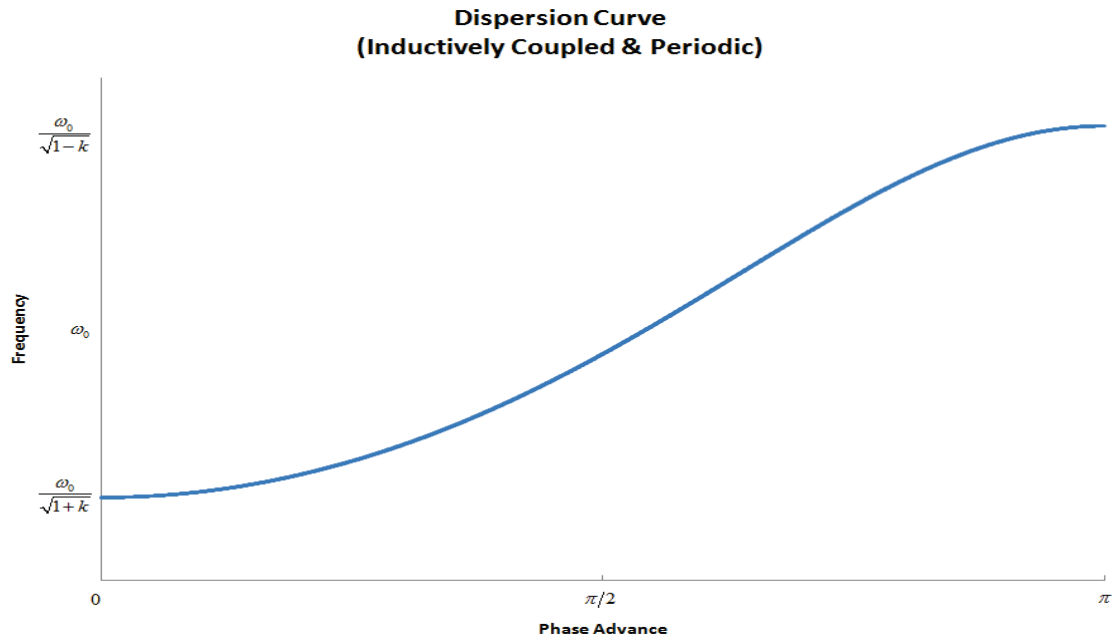

Figure 3-3: The dispersion curve for an inductively coupled, periodic, standing wave structure of N resonant cavities, given by Eq. (3.13). This curve is typical referred to as a "Brillouin curve" in reference to Léon Brillouin for his related work in solid state physics [Bri 46].

Fig. (3-3) shows that for any given structure the $\pi/2$ mode will have the most mode separation of any of the other normal modes, whereas both the 0-mode and the π-mode will have the least.

3.2 Inductively Coupled Biperiodic Standing Wave Structure

Fig. (3-4) shows an on-axis inductively coupled biperiodic structure. However, no distinction in the circuit equivalent model between on-axis and off-axis coupling is required, and the model will work equally well for either.

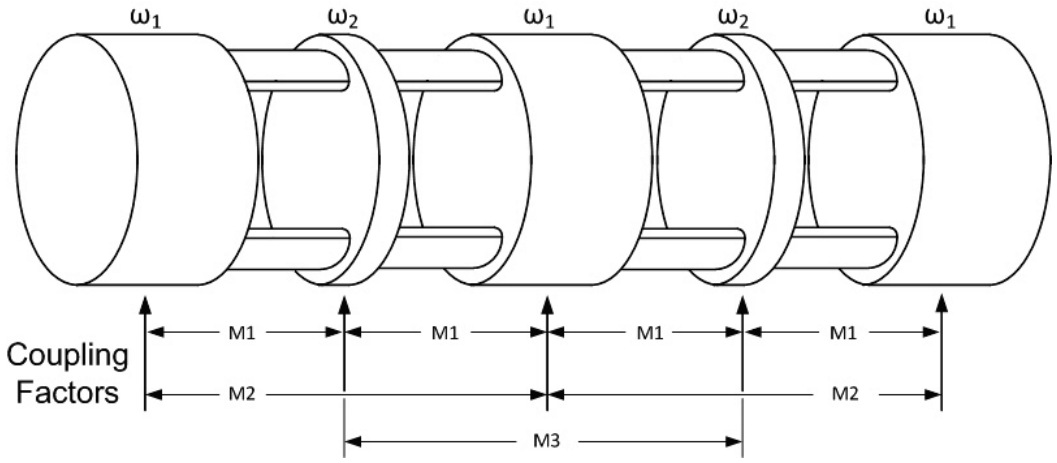

Figure 3-4: Coupled resonator model for a biperiodic chain of cavities with nearest neighbor and second nearest neighbor coupling.

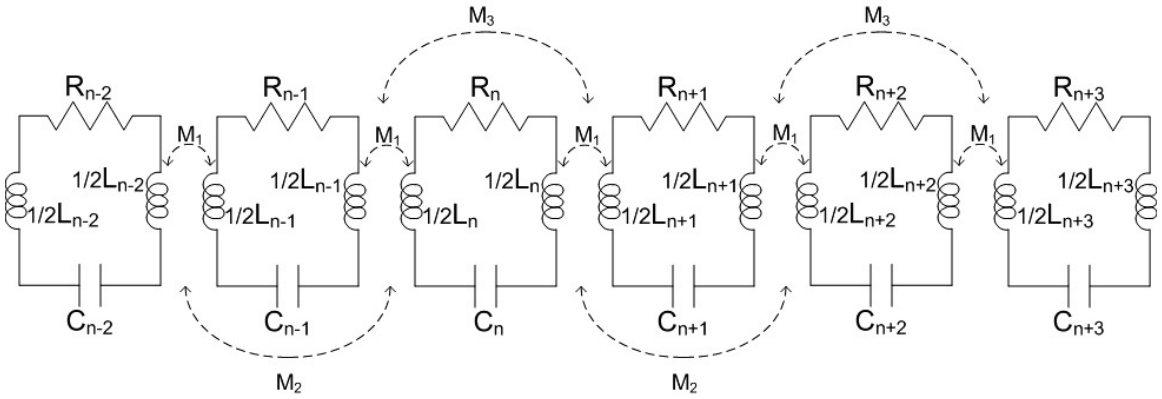

Figure 3-5: Equivalent circuit model for an inductively coupled, biperiodic, standing wave structure with N cavities. This model includes nearest and next nearest neighbor coupling.

Fig. (3-4) shows that model is now allowing for next nearest neighbor coupling. Next nearest neighbor coupling means that the current in cavity *N* will affect the current in cavities *N*-2, and *N*+2. It's worth noting that some accelerating structures might not need to include next nearest neighbor coupling in order to find good agreement with

experimental results, and others might need to include next next nearest neighboring coupling, depending on the coupling that particular accelerating structure.

In this model the n^{th} cell is an a-cell and every other (as in alternating) cell before and after it is identical, each with a resonant frequency equal to ω_1. The $n^{th}+1$ cell is a c-cell and every other (also as in alternating) cell before and after it is identical, each with a resonant frequency equal to ω_2.

Using Kirchhoff's loop in the n^{th} and $n^{th}+1$ tank circuit yields the following relationships.

$$0 = i_n\left(j\omega L_n + R_n + \frac{1}{j\omega C_n}\right) + M_1 j\omega L_n\left(i_{n-1} + i_{n+1}\right) + M_2 j\omega L_n\left(i_{n-2} + i_{n+2}\right) \tag{3.15}$$

$$0 = i_{n+1}\left(j\omega L_{n+1} + R_{n+1} + \frac{1}{j\omega C_{n+1}}\right) + M_1 j\omega L_{n+1}\left(i_n + i_{n+2}\right) + M_3 j\omega L_{n+1}\left(i_{n-1} + i_{n+3}\right) \tag{3.16}$$

(3.15) is divide by $jL_n\omega$, (3.16) is divided by $jL_{n+1}\omega$, and $M_1 = \frac{k_1}{2}$, $M_2 = \frac{k_2}{2}$, $M_3 = \frac{k_3}{2}$

$$0 = i_n\left(1 + \frac{R_n}{j\omega L_n} - \frac{1}{\omega^2 L_n C_n}\right) + \frac{k_1}{2}\left(i_{n-1} + i_{n+1}\right) + \frac{k_2}{2}\left(i_{n-2} + i_{n+2}\right) \tag{3.17}$$

$$0 = i_{n+1}\left(1 + \frac{R_n}{j\omega L_n} - \frac{1}{\omega^2 L_n C_n}\right) + \frac{k_1}{2}\left(i_n + i_{n+2}\right) + \frac{k_3}{2}\left(i_{n-1} + i_{n+3}\right) \tag{3.18}$$

Using (2.5) and (2.7) from the tank circuit section.

$$\omega_1 = \frac{1}{\sqrt{L_n C_n}} \quad \text{and} \quad Q_1 = \frac{\omega_n L_n}{R_n}$$

$$\omega_2 = \frac{1}{\sqrt{L_{n+1} C_{n+1}}} \quad \text{and} \quad Q_2 = \frac{\omega_{n+1} L_{n+1}}{R_{n+1}}$$

$$0 = i_n\left(1+\frac{\omega_1}{\omega jQ_1}-\frac{\omega_1^2}{\omega^2}\right)+\frac{k_1}{2}\left(i_{n-1}+i_{n+1}\right)+\frac{k_2}{2}\left(i_{n-2}+i_{n+2}\right) \tag{3.19}$$

$$0 = i_{n+1}\left(1+\frac{\omega_2}{\omega jQ_2}-\frac{\omega_2^2}{\omega^2}\right)+\frac{k_1}{2}\left(i_n+i_{n+2}\right)+\frac{k_3}{2}\left(i_{n-1}+i_{n+3}\right) \tag{3.20}$$

As before, the problem is simplified by assuming the cavities are lossless.

$$0 = i_n\left(1-\frac{\omega_1^2}{\omega^2}\right)+\frac{k_1}{2}\left(i_{n-1}+i_{n+1}\right)+\frac{k_2}{2}\left(i_{n-2}+i_{n+2}\right) \tag{3.21}$$

$$0 = i_{n+1}\left(1-\frac{\omega_2^2}{\omega^2}\right)+\frac{k_1}{2}\left(i_n+i_{n+2}\right)+\frac{k_3}{2}\left(i_{n-1}+i_{n+3}\right) \tag{3.22}$$

Since the structure is now biperiodic the assumed solution will allow the amplitude to differ between the two types of cavities; however every cavity of the same type is assumed to have the same amplitude.

$$i_n(q) = A\cos\left(n\varphi\right)e^{j\omega_q t} \tag{3.23}$$

$$i_{n+1}(q) = B\cos\left[\left(n+1\right)\varphi\right]e^{j\omega_q t} \tag{3.24}$$

Where $\varphi = \dfrac{\pi q}{N-1}$, $0 \geq q \leq (N-1)$, and $1 \geq n \leq N$

Substituting (3.23) and (3.24) into (3.21) yields (3.25)

$$\begin{aligned} 0 = A\cos\left(n\varphi\right)\cdot\left(1-\frac{\omega_1^2}{\omega^2}\right)+\frac{k_1}{2}\left\{B\cos\left[\left(n-1\right)\varphi\right]+B\cos\left[\left(n+1\right)\varphi\right]\right\} \\ +\frac{k_2}{2}\left\{A\cos\left[\left(n-2\right)\varphi\right]+A\cos\left[\left(n+2\right)\varphi\right]\right\} \end{aligned} \tag{3.25}$$

Substituting (3.23) and (3.24) into (3.22) yields (3.26)

$$\begin{aligned} 0 = B\cos\left[\left(n+1\right)\varphi\right]\cdot\left(1-\frac{\omega_2^2}{\omega^2}\right)+\frac{k_1}{2}\left\{A\cos\left(n\varphi\right)+A\cos\left[\left(n+2\right)\varphi\right]\right\} \\ +\frac{k_3}{2}\left\{B\cos\left[\left(n-1\right)\varphi\right]+B\cos\left[\left(n+3\right)\varphi\right]\right\} \end{aligned} \tag{3.26}$$

(3.27), (3.28), (3.29), (3.30) Make extensive use of (3.12)

$$\frac{k_1}{2}\left\{B\cos\left[(n-1)\varphi\right]+B\cos\left[(n+1)\varphi\right]\right\}=\frac{k_1 B}{2}\left[\cos(n\varphi-\varphi)+\cos(n\varphi+\varphi)\right] \\ =k_1 B\cos(n\varphi)\cos(\varphi) \tag{3.27}$$

$$\frac{k_2}{2}\left\{A\cos\left[(n-2)\varphi\right]+A\cos\left[(n+2)\varphi\right]\right\}=\frac{k_2 A}{2}\left[\cos(n\varphi-2\varphi)+\cos(n\varphi+2\varphi)\right] \\ =k_2 A\cos(n\varphi)\cos(2\varphi) \tag{3.28}$$

$$\frac{k_1}{2}\left\{A\cos\left[n\varphi\right]+A\cos\left[(n+2)\varphi\right]\right\}=\frac{k_1 A}{2}\left\{\cos\left[(n+1)\varphi-\varphi\right]+\cos\left[(n+1)\varphi+\varphi\right]\right\} \\ =k_1 A\cos\left[(n+1)\varphi\right]\cos(\varphi) \tag{3.29}$$

$$\frac{k_3}{2}\left\{B\cos\left[(n-1)\varphi\right]+B\cos\left[(n+3)\varphi\right]\right\}=\frac{k_3 B}{2}\left\{\cos\left[(n+1)\varphi-2\varphi\right]+\cos\left[(n+1)\varphi+2\varphi\right]\right\} \\ =k_3 B\cos\left[(n+1)\varphi\right]\cos(2\varphi) \tag{3.30}$$

Substituting (3.27) and (3.28) into (3.25). Then (3.29) and (3.30) into (3.26).

$$0=A\left(1-\frac{\omega_1^2}{\omega^2}\right)+k_1 B\cos(\varphi)+k_2 A\cos(2\varphi) \tag{3.31}$$

$$0=B\left(1-\frac{\omega_2^2}{\omega^2}\right)+k_1 A\cos(\varphi)+k_3 B\cos(2\varphi) \tag{3.32}$$

Solving (3.32) for B

$$B=\frac{-k_1 A\cos(\varphi)}{1-\frac{\omega_2^2}{\omega^2}+k_3\cos(2\varphi)} \tag{3.33}$$

Substituting (3.33) into (3.31)

$$k_1^2\cos^2(\varphi)=1-\frac{\omega_2^2}{\omega^2}+k_3\cos(2\varphi)-\frac{\omega_1^2}{\omega^2}+\frac{\omega_1^2\omega_2^2}{\omega^2}+\frac{\omega_1^2}{\omega^2}k_3\cos(2\varphi) \\ +k_2\cos(2\varphi)-\frac{\omega_2^2}{\omega^2}k_2\cos(2\varphi)+k_2k_3\cos^2(2\varphi) \tag{3.34}$$

Factoring (3.34) yields (3.35) the familiar form of the dispersion relationship.

$$\boxed{k_1^2\cos^2\varphi=\left(1-\omega_1^2/\omega^2+k_2\cos 2\varphi\right)\times\left(1-\omega_2^2/\omega^2+k_3\cos 2\varphi\right)} \tag{3.35}$$

In Eq. (3.35) ω is to the 4th power, resulting in two possible mathematical solutions for the dispersion relationship: one of these solutions corresponding to the positive root of the quadratic(3.39), and the other corresponding to the negative root (3.40).

$$a = k_1^2 \cos^2(\varphi) - k_2 \cos(2\varphi) - k_3 \cos(2\varphi) - k_2 k_3 \cos^2(2\varphi) - 1 \tag{3.36}$$

$$b = \omega_2^2 + \omega_1^2 + \omega_2^2 k_2 \cos(2\varphi) - \omega_1^2 k_3 \cos(2\varphi) \tag{3.37}$$

$$c = \omega_1^2 \omega_2^2 \tag{3.38}$$

$$\omega_+ = \sqrt{\frac{-b + \sqrt{b^2 - 4ac}}{2a}} \tag{3.39}$$

$$\omega_- = \sqrt{\frac{-b - \sqrt{b^2 - 4ac}}{2a}} \tag{3.40}$$

Both (3.39) and (3.40) are symmetric about $\varphi = \pi/2$ and difference between them at $\varphi = \pi/2$ is known as the stopband (SB). This problem is very similar to Brillouin's treatment of a one-dimensional NaCl Lattice, where he used the term "stopping band" [Bri 46]. The Los Alamos group used the term "stopband", and that seems to be the phrasing which stuck.

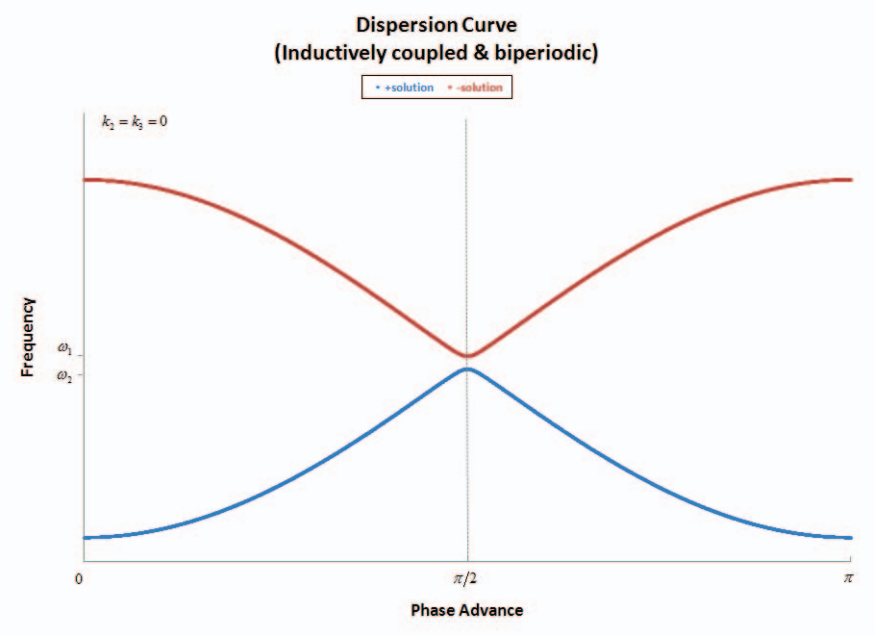

Figure 3-6: Dispersion curve obtained from (3.39) and (3.40) with (k_2=k_3=0) which is equivalent to saying no next nearest neighbor coupling.

The physical solution is actually a combination of both mathematical solutions. One root describes the structure between 0 and $\pi/2$ phase advance, and the other root describes the structure between $\pi/2$ and π as shown on Fig. (3-7).

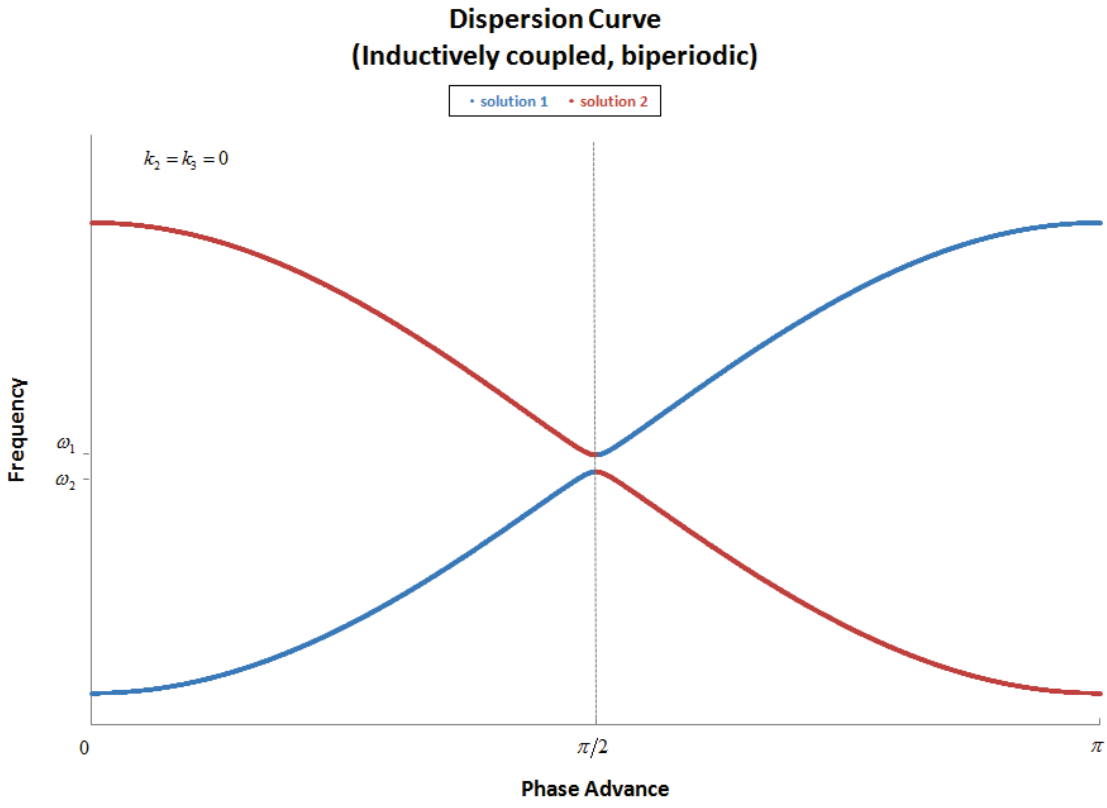

Figure 3-7: For any given structure only 1 of these solutions is possible at any given time. The frequency range of the solution in the region of $\pi/2 < \varphi \leq \pi$ is referred to as the "upper pass band", and as the "lower pass band" in the region of $0 \geq \varphi < \pi/2$ is. The "stopband" occurs at $\varphi = \pi/2$ and is equal Eq. (3.41).

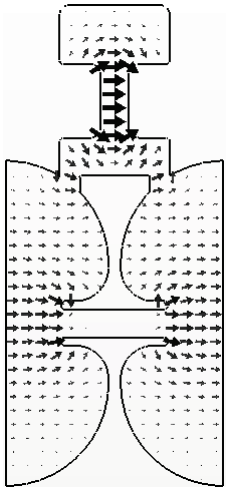

Figure 3-8: Lowest normal mode in a 3 cavity inductively coupled biperiodic off-axis standing wave accelerator exhibiting 0 phase advance as in solution 1 from fig. (3-7).

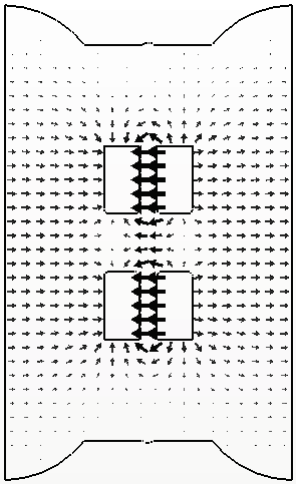

Figure 3-9: Lowest normal mode in a 3 cavity inductively coupled biperiodic on-axis standing wave accelerator exhibiting π phase advance as in solution 2 from fig. (3-7).

Fig. (3-8) shows the Los Alamos's "model K" type biperiodic structure [Kap 68]. Their results agree with solution 1 in Fig. (3-7). Fig. (3-9) shows a biperiodic structure proposed by several different groups. One example, is a proposed c-band accelerator presented at PAC07 [KIM 07]. This group's results agree with solution 2 in Fig. (3-7). Note that both biperiodic structure shown in figures 3-8 and 3-9 make use of inductive coupling but the geometry of the coupling slots and coupling cavity's dimensions determines which solution is correct for their dispersion relationship.

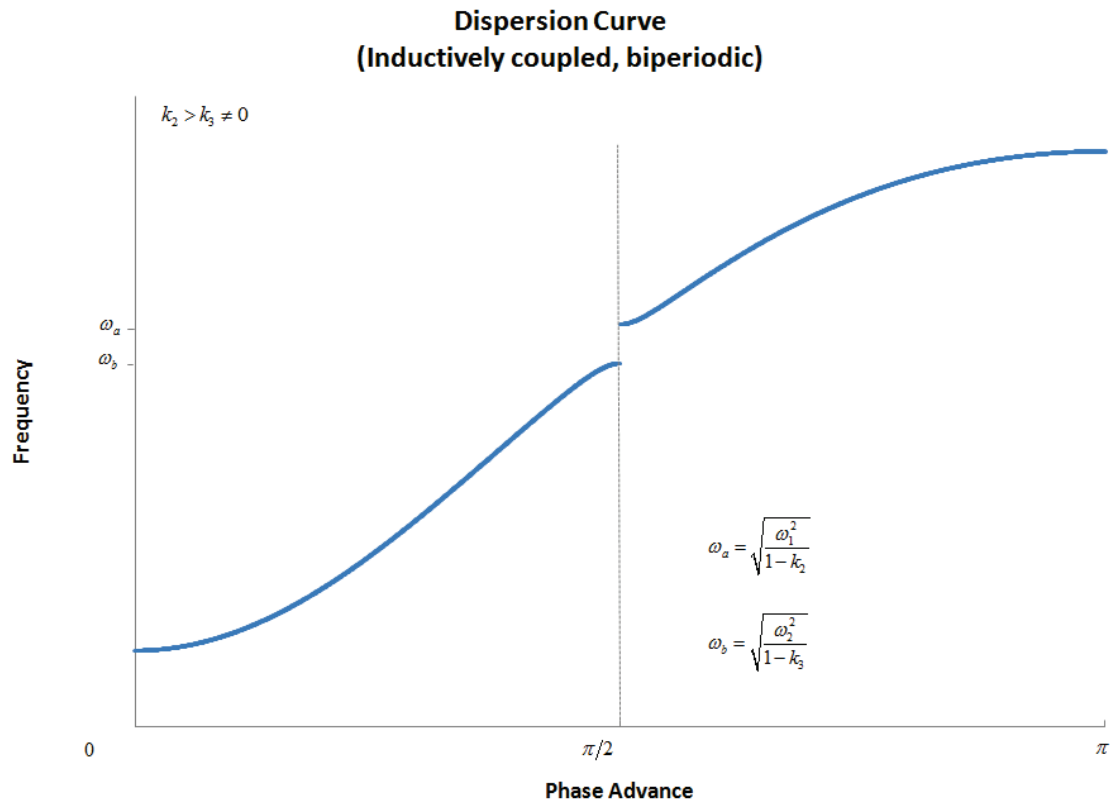

Figure 3-10: Dispersion curve obtained from (3.35) with next nearest neighbor coupling included. In this plot k_3 is twice as large as k_2 and $\omega_1 > \omega_2$. Only one solution is shown for clarity.

The stopband neglecting losses for an inductively coupled biperiodic standing-wave accelerator is equal to (3.41).

$$\text{stopband} = \frac{f_2}{\sqrt{1-k_3}} - \frac{f_1}{\sqrt{1-k_2}} \tag{3.41}$$

Remember at the beginning of the section ω_1 was defined as the resonant frequency of the a-cells and ω_2 was defined as the resonant frequency of the c-cells. Stopband is often referred to as an absolute value. I have found that is useful to always subtract the c-cell frequency from the a-cell frequency and leave the sign in the stopband value. This way, if you say you have a stopband of 10MHz, it's known that the c-ells are 10MHz higher in

frequency than the a-cells. In chapter 5 I'll show that the sign of the stopband is significant in determining the direction of field slope when an a-cell is mistuned.

3.3 Capacitively Coupled Periodic Standing Wave Structure

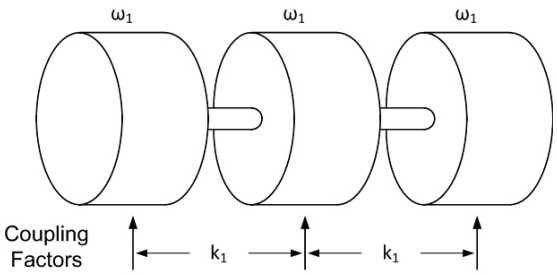

3-11: Periodic capacitively coupled standing wave structure.

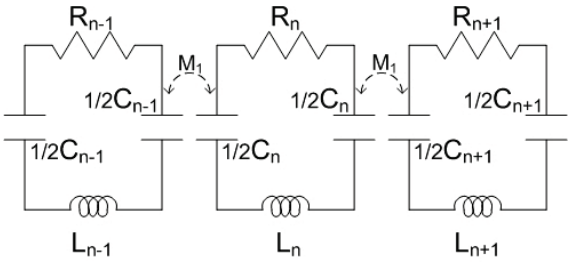

3-12: Equivalent circuit model of Fig (3-11).

The circuit equivalent model for this structure consists of N tank circuits coupled together via mutual capacitance. As before, with the inductively coupled periodic structure in section 3.1, only nearest neighbor coupling will be considered. So mutual capacitance will only exist between adjacent cavities.

Using Kirchhoff's loop in the n^{th} tank circuit yields the following relationship.

$$0 = i_n R_n + \frac{\int_0^t i_n(\tau)\,d\tau}{C_n} + L_n \frac{di_n}{dt} + M_1 \frac{\int_0^t i_{n-1}(\tau)\,d\tau}{C_n} + M_1 \frac{\int_0^t i_{n+1}(\tau)\,d\tau}{C_n} \qquad (3.42)$$

M_1 is a unit less coupling constant defined in way similar to how it was in the previous sections, where $\frac{M_1}{C_n}\int_0^t i_{n-1}(\tau)\,d\tau$ is the voltage created across $C_n = 1/2\,C_n + 1/2\,C_n = C_{eff}$ when the current in cell n-1 changes with respect to time. Each cavity is identical, so the coupling between adjacent cavities will be the same. The Laplace transform equations (3.2) and (3.3) are used, and the following substitution is made $s = j\omega$.

$$0 = i_n\left(j\omega L_n + R_n + \frac{1}{j\omega C_n}\right) + \frac{i_{n-1}M_1}{j\omega C_n} + \frac{i_{n+1}M_1}{j\omega C_n} \qquad (3.43)$$

Notice the only difference between (3.5) and (3.43) is in the coupling terms as one would expect. Next, Divide by $jL_n\omega$ and let $M_1 = \frac{k_1}{2}$.

$$0 = i_n\left(1+\frac{R_n}{\omega jL_n}-\frac{1}{\omega^2 L_n C_n}\right)-\frac{k_1}{2}\left(\frac{i_{n-1}}{\omega^2 C_n L_n}+\frac{i_{n+1}}{\omega^2 C_n L_n}\right) \tag{3.44}$$

Using the relations described in the tank circuit section as in previous sections.

$$0 = i_n\left(1+\frac{\omega_n}{\omega jQ_n}-\frac{\omega_n^2}{\omega^2}\right)+\frac{k_1}{2}\left(i_{n-1}\frac{\omega_n^2}{\omega^2}+i_{n+1}\frac{\omega_n^2}{\omega^2}\right) \tag{3.45}$$

The structure is assumed to be lossless so Q becomes infinite. And, since all the cavities are identical, the following substation is made $\omega_n = \omega_0$.

$$0 = i_n\left(1-\frac{\omega_0^2}{\omega^2}\right)+\frac{k_1\omega_0^2}{2\omega^2}\left(i_{n-1}+i_{n+1}\right) \tag{3.46}$$

The solution for the current in the n^{th} cell (3.9) will be the same as it was in the periodic inductively coupled case. The same arguments used as motivation in that problem hold in this case as well. Substituting Eq. (3.9) into (3.46)

$$0 = \left(1-\frac{\omega_0^2}{\omega^2}\right)\cos\left(\frac{\pi qn}{N-1}\right)-\frac{k_1\omega_n^2}{2\omega^2}\left[\cos\left(\frac{\pi q}{N-1}(n-1)\right)+\cos\left(\frac{\pi q}{N-1}(n+1)\right)\right] \tag{3.47}$$

After dividing out the exponential factor and the constant A, let $a = \frac{\pi qn}{N-1}$, $b = \frac{\pi q}{N-1}$, and make use of (3.12)

$$0 = \left(1-\frac{\omega_0^2}{\omega^2}\right)\cos\left(a\right)+\frac{k_1\omega_n^2}{2\omega^2}\left[\cos\left(a-b\right)+\cos\left(a+b\right)\right] \tag{3.48}$$

The dispersion relationship for a capacitively coupled periodic resonant cavity chain is given by.

$$\boxed{\omega^2 = \omega_0^2\left[1 + k_1 \cos\left(\frac{\pi q}{N-1}\right)\right]} \tag{3.49}$$

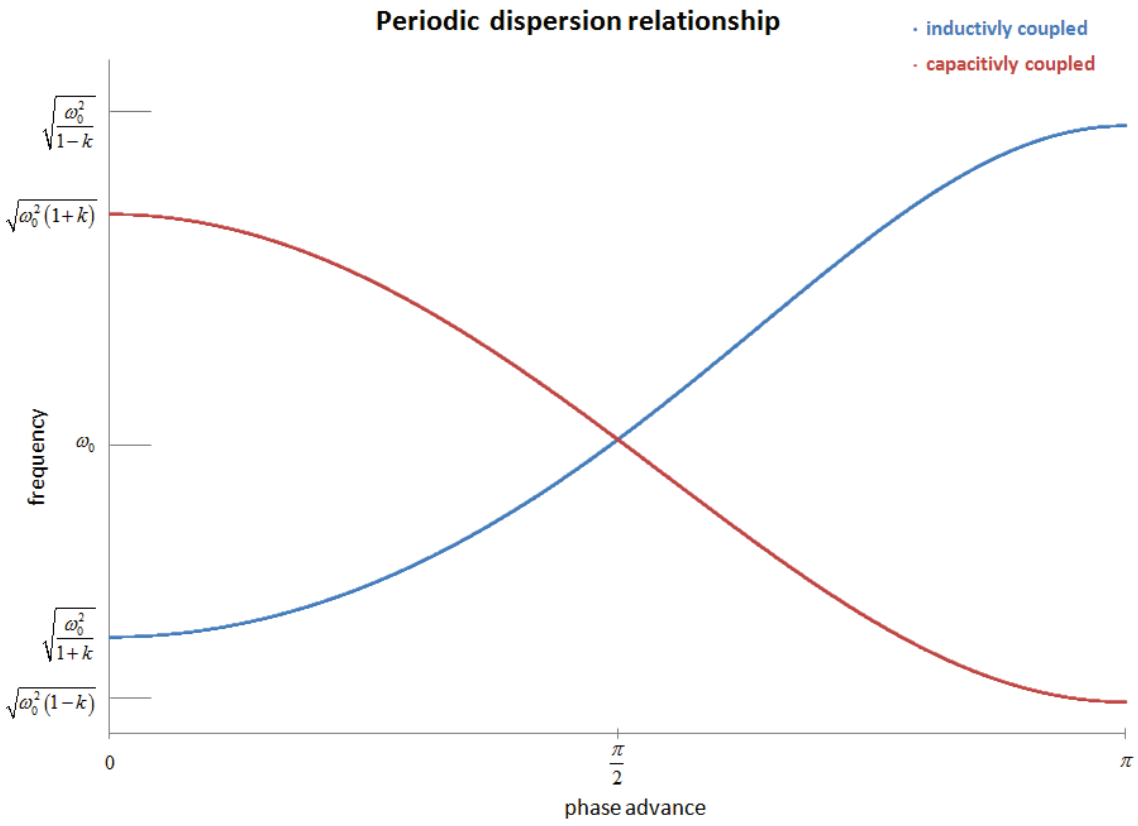

Figure 3-13: Comparison of an inductively coupled periodic structure vs. a capacitively coupled periodic structure.

The major difference between the two curves is that the curve corresponding to inductive coupling experiences a maxima at $\varphi = \pi$ and a minima at $\varphi = 0$. Whereas the curve corresponding to capacitive coupling experiences a minima at $\varphi = 0$, and a maxima at $\varphi = \pi$. Besides this inversion about ω_0, the curves also have a slightly different dependence on *k*. However, for small *k* values this difference is small.

3.4 Capacitively Coupled Biperiodic Standing Wave Structure

The derivation of this structure's dispersion equation (3.64) is very similar to how (3.35) was derided in section 3.2. The coupling terms are defined in the previous section.

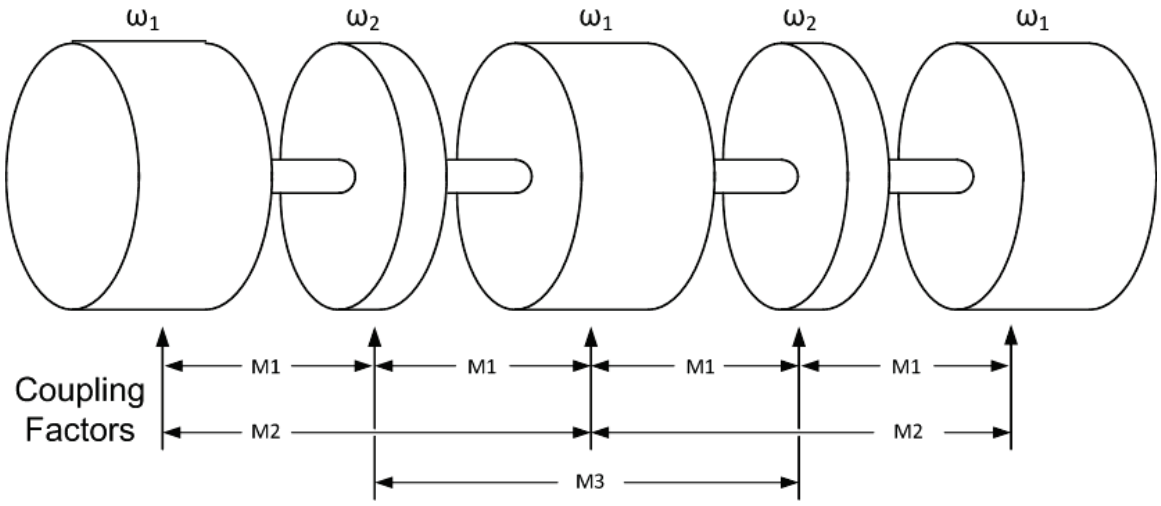

Figure 3-14: Coupled resonator model for a biperiodic chain of cavities with nearest neighbor and second nearest neighbor capacitive coupling.

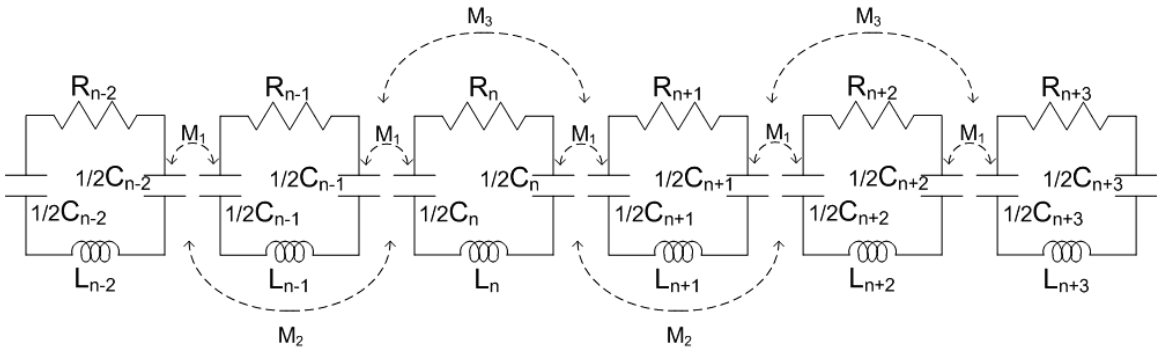

Figure 3-15: Circuit equivalent model for a capacitively coupled, biperiodic, standing wave structure with N cavities. This model includes nearest and next nearest neighbor coupling.

Using Kirchhoff's loop in the n^{th} and $n^{th}+1$ tank circuit yields the following relationships.

$$0 = i_n\left(j\omega L_n + R_n + \frac{1}{j\omega C_n}\right) + \frac{M_1}{j\omega C_n}\left(i_{n-1} + i_{n+1}\right) + \frac{M_2}{j\omega C_n}\left(i_{n-2} + i_{n+2}\right) \tag{3.50}$$

$$0 = i_{n+1}\left(j\omega L_{n+1} + R_{n+1} + \frac{1}{j\omega C_{n+1}}\right) + \frac{M_1}{j\omega C_{n+1}}\left(i_n + i_{n+2}\right) + \frac{M_3}{j\omega C_{n+1}}\left(i_{n-1} + i_{n+3}\right) \tag{3.51}$$

Divide (3.50) by $jL_n\omega$ and (3.51) by $jL_{n+1}\omega$ then let $M_1 = \frac{k_1}{2}$, $M_2 = \frac{k_2}{2}$, and $M_3 = \frac{k_3}{2}$ in both (3.52) and (3.53).

$$0 = i_n\left(1 + \frac{R_n}{j\omega L_n} - \frac{1}{\omega^2 L_n C_n}\right) - \frac{k_1}{2\omega^2 L_n C_n}\left(i_{n-1} + i_{n+1}\right) - \frac{k_2}{2\omega^2 L_n C_n}\left(i_{n-2} + i_{n+2}\right) \tag{3.52}$$

$$0 = i_{n+1}\left(1 + \frac{R_{n+1}}{j\omega L_{n+1}} - \frac{1}{\omega^2 L_{n+1} C_{n+1}}\right) - \frac{k_1}{2\omega^2 L_{n+1} C_{n+1}}\left(i_n + i_{n+2}\right) + \frac{k_3}{2\omega^2 L_{n+1} C_{n+1}}\left(i_{n-1} + i_{n+3}\right) \tag{3.53}$$

Using the relations described in the tank circuit section, and simplifying the problem by assuming cavities are lossless.

$$\omega_1 = \frac{1}{\sqrt{L_n C_n}} \quad \text{and} \quad \omega_2 = \frac{1}{\sqrt{L_{n+1} C_{n+1}}}$$

$$0 = i_n\left(1 - \frac{\omega_1^2}{\omega^2}\right) - \frac{\omega_1^2 k_1}{2\omega^2}\left(i_{n-1} + i_{n+1}\right) - \frac{\omega_1^2 k_2}{2\omega^2}\left(i_{n-2} + i_{n+2}\right) \tag{3.54}$$

$$0 = i_{n+1}\left(1 - \frac{\omega_2^2}{\omega^2}\right) - \frac{\omega_2^2 k_1}{2\omega^2}\left(i_n + i_{n+2}\right) - \frac{\omega_2^2 k_3}{2\omega^2}\left(i_{n-1} + i_{n+3}\right) \tag{3.55}$$

The assumed solution for the current in the nth cell (3.56) and in the nth+1 cell (3.57) is the same as it was in the biperiodic inductively coupled case.

$$i_n(q) = A\cos\left(n\varphi\right)e^{j\omega_q t} \tag{3.56}$$

$$i_{n+1}(q) = B\cos\left[\left(n+1\right)\varphi\right]e^{j\omega_q t} \tag{3.57}$$

Where $\varphi = \frac{\pi q}{N-1}$, $0 \geq q \leq (N-1)$, and $1 \geq n \leq N$

Substituting (3.56) and (3.57) into (3.54) and then dividing out the exponential term.

$$0 = A\cos(n\varphi)\cdot\left(1-\frac{\omega_1^2}{\omega^2}\right)-\frac{\omega_1^2 k_1}{2\omega^2}\left\{B\cos\left[(n-1)\varphi\right]+B\cos\left[(n+1)\varphi\right]\right\} \\ -\frac{\omega_1^2 k_2}{2\omega^2}\left\{A\cos\left[(n-2)\varphi\right]+A\cos\left[(n+2)\varphi\right]\right\} \tag{3.58}$$

Substituting (3.56) and (3.57) into (3.55) and then dividing out the exponential term.

$$0 = B\cos\left[(n+1)\varphi\right]\cdot\left(1-\frac{\omega_1^2}{\omega^2}\right)-\frac{\omega_2^2 k_1}{2\omega^2}\left\{A\cos(n\varphi)+A\cos\left[(n+2)\varphi\right]\right\} \\ -\frac{\omega_2^2 k_3}{2\omega^2}\left\{B\cos\left[(n-1)\varphi\right]+B\cos\left[(n+3)\varphi\right]\right\} \tag{3.59}$$

Substituting (3.27) and (3.28) into (3.58)

$$0 = A\left(1-\frac{\omega_1^2}{\omega^2}\right)-\frac{\omega_1^2 k_1}{\omega^2}B\cos(\varphi)-\frac{\omega_1^2 k_2}{\omega^2}A\cos(2\varphi) \tag{3.60}$$

Substituting (3.29) and (3.30) into (3.59)

$$0 = B\left(1-\frac{\omega_2^2}{\omega^2}\right)-\frac{\omega_2^2 k_1}{\omega^2}A\cos(\varphi)-\frac{\omega_2^2 k_3}{\omega^2}B\cos(2\varphi) \tag{3.61}$$

Solving (3.61) for B

$$B = \frac{\frac{\omega_2^2 k_1}{\omega^2}A\cos(\varphi)}{1-\frac{\omega_2^2}{\omega^2}-\frac{\omega_2^2 k_3}{\omega^2}\cos(2\varphi)} \tag{3.62}$$

$$\frac{\omega_1^2\omega_2^2}{\omega^4}k_1^2\cos^2(\varphi) = 1-\frac{\omega_2^2}{\omega^2}-\frac{\omega_2^2 k_3}{\omega^2}\cos(2\varphi)-\frac{\omega_1^2}{\omega^2}+\frac{\omega_1^2\omega_2^2}{\omega^4}+\frac{\omega_1^2\omega_2^2 k_3}{\omega^4}\cos(2\varphi) \\ -\frac{\omega_1^2 k_2}{\omega^2}\cos(2\varphi)+\frac{\omega_1^2\omega_2^2 k_2}{\omega^4}\cos(2\varphi)+\frac{\omega_1^2\omega_2^2 k_2 k_3}{\omega^4}\cos^2(2\varphi) \tag{3.63}$$

After simplifying Eq. (3.63) by factoring, canceling common terms, and pulling out negative sings; the biperiodic capacitively coupled dispersion equation is given by Eq. (3.64).

$$\boxed{k_1^2\cos^2\varphi = \left(1-\omega^2/\omega_1^2+k_2\cos 2\varphi\right)\times\left(1-\omega^2/\omega_2^2+k_3\cos 2\varphi\right)} \tag{3.64}$$

As was the case in the biperiodic inductively coupled dispersion, Eq. (3.64) has two mathematical solutions, and the two possible physical solutions are again combinations of both mathematical solutions. However, the dispersion Eqs. (3.64) and (3.35) differ in which roots are used to produce the physical solutions. This can be seen in Fig. (3-16) by which cavity type (a-cell or c-cell) determines the value of the lower pass band frequency at $\varphi = \pi/2$. In the capacitively coupled case it's ω_1 the a-cell, and in the inductively coupled case it's ω_2 the c-cell. This is in agreement with the work published by a group at the Institute of Nuclear Power in Poland in 1985 [Sek 85].

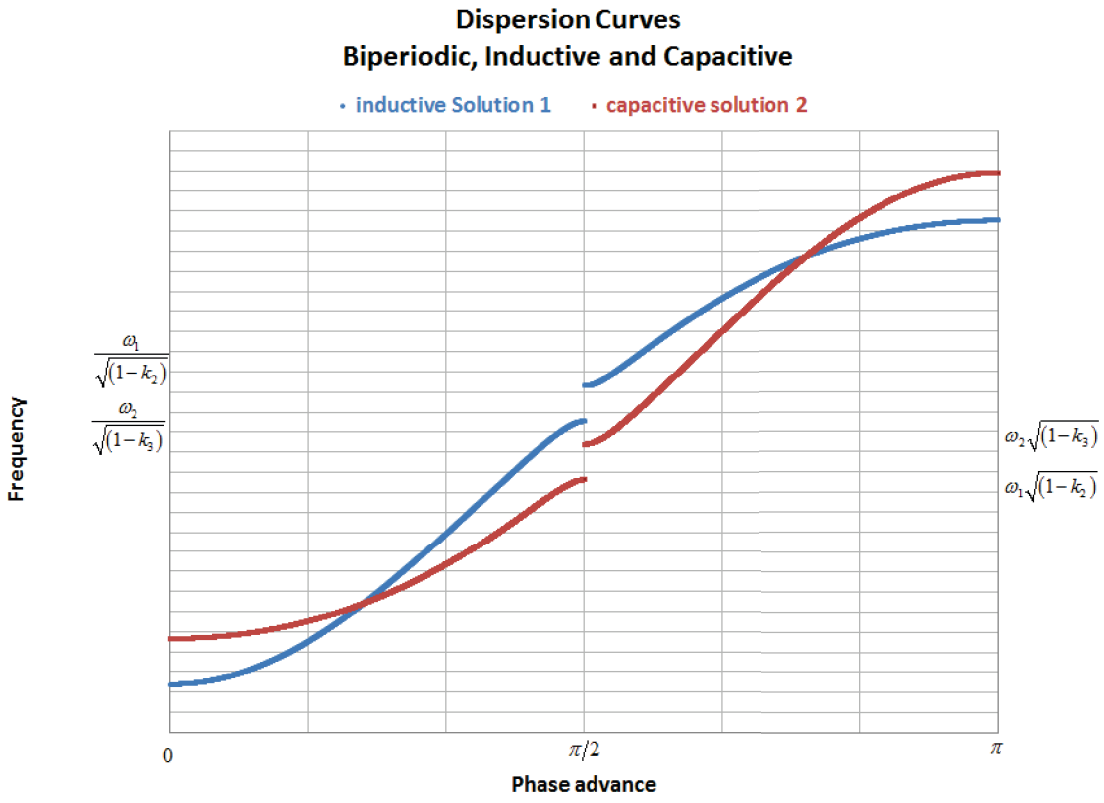

Figure 3-16: Comparison of inductive vs. capacitive coupled biperiodic dispersion curves with stopband. Only the solution where the lowest frequency normal mode is the 0-made is shown in both cases.

Their paper included a review of the biperiodic inductively coupled dispersion equation derived at Los Alamos [Nag 67]. They found that which cavity type a-cell (ω_1) or c-cell (ω_2) determines the value of the lower pass band frequency (at $\varphi = \pi/2$) depends on the sign of the nearest neighbor coupling term (k_{ab} in their notation). Fig.2 in their publication shows that when k_{ab} (k_1 in our notation) is negative f_a (ω_1) is used, and when k_{ab} is positive f_b (ω_2) is used. A negative k_{ab} (k_1) term implies the nearest neighbor coupling is predominantly capacitive if the model was derived using inductive coupling. This is because of the phase difference between inductive and capacitive reactance.

The stopband of capacitively coupled biperiodic standing wave structure is given by Eq.(3.65).

$$\text{stopband} = f_2\sqrt{1-k_3} - f_1\sqrt{1-k_2} \tag{3.65}$$

3.5 Determining Dispersion Parameters, the "five mode" Method.

In order to make use of the dispersion equation derived in sections 3.2 and 3.4, a method is needed for determining k_1, k_2, k_3, f_1, and f_2. This can be done by measuring at least 5 normal modes of a given standing wave structure. The group from the Institute of Nuclear Power in Poland published this "five mode" method using Eq.(3.35) as the dispersion equation, as well as using a dispersion equation they derived from a circuit equivalent model which had both inductive and capacitive coupling at the same time [Sek 85]. Despite this papers existence, four years later, a group in India was unable to find an analytic 5 mode method using equation Eq.(3.35) as the dispersion equation, and published a method for determining the coupling coefficients using fitting techniques [Sha 89]. More recently another group from Institute of Nuclear Power in Poland presented another analytic solution using Eq.(3.35) as the dispersion equation at PAC09 [Kul 09].

This chapter shows a five mode method for the biperiodic capacitively coupled dispersion equation given by Eq.(3.64). For its 5 normal modes, it makes use of the 0, $\pi/4$, $\pi/2$, $3\pi/4$, and π normal modes frequencies.

After measuring f_0, $f_{\pi/4}$, $f_{\pi/2}$, $f_{3\pi/4}$, and f_π of at least five capacitively coupled biperiodic cavities. Eq. (3.64) can be rewritten as Eqs. (3.66) through (3.70).

$$\left(1-\frac{f_0^2}{f_1^2}+k_2\right)\left(1-\frac{f_0^2}{f_2^2}+k_3\right)=k_1^2 \tag{3.66}$$

$$\left(1-\frac{f_{\pi/4}^2}{f_1^2}\right)\left(1-\frac{f_{\pi/4}^2}{f_2^2}\right)=\frac{1}{2}k_1^2 \tag{3.67}$$

$$\left(1-\frac{f_{\pi/2}^2}{f_1^2}-k_2\right)\left(1-\frac{f_{\pi/2}^2}{f_2^2}-k_3\right)=0 \tag{3.68}$$

$$\left(1-\frac{f_{3\pi/4}^2}{f_1^2}\right)\left(1-\frac{f_{3\pi/4}^2}{f_2^2}\right)=\frac{1}{2}k_1^2 \tag{3.69}$$

$$\left(1-\frac{f_\pi^2}{f_1^2}+k_2\right)\left(1-\frac{f_\pi^2}{f_2^2}+k_3\right)=k_1^2 \tag{3.70}$$

Eqs. (3.66) through (3.70) are five nonlinear coupled equations with 5 unknowns. The problem is to solve for the five unknown terms in terms of the five measured frequencies. This problem is a little trickier than it sounds.

The first consideration when solving this problem is how $f_{\pi/2}$ was measured. More specifically, what boundary conditions were used when it was measured. Boundary conditions will dictate whether the π/2 normal mode will be located in the accelerating cavities or in the coupling cavities. The former is the most common, as it is created easily by terminating half of an a-cell with an electrical boundary. Fig. (4-2) shows this type of test set up. In the case depicted by Fig. (4-2), the correct solution to Eq. (3.68) is Eq. (3.71).

$$f_{\pi/2}=f_1\sqrt{1-k_2} \tag{3.71}$$

However, alternative boundary conditions have been proposed which would allow one to measure the π/2 normal mode centered in coupling cavities [Yan 10]. None of the math shown here would apply to such a measurement. All equations in this section assume that all frequencies were measured with the π/2 normal mode located in the a-cells.

The couple between a-cells (k_2) is then given by Eq. (3.72).

$$\boxed{k_{2\pm} = \frac{-B \pm \sqrt{B^2 - 4AC}}{2A}} \tag{3.72}$$

For our relatively narrow-band structures, C<<1 with the result that k_{2-} is negative of order unity, while k_{2+}, is small and positive. The correct root is k_{2+}, where A, B, and C are given by (3.73), (3.74), and (3.75).

$$A = \left(1 + \frac{f_0^2}{f_{\pi/2}^2}\right)\left(1 + \frac{f_\pi^2}{f_{\pi/2}^2}\right) - 2\frac{f_{\pi/4}^2 f_{3\pi/4}^2}{f_{\pi/2}^4} \tag{3.73}$$

$$B = \left(1 + \frac{f_0^2}{f_{\pi/2}^2}\right)\left(1 - \frac{f_\pi^2}{f_{\pi/2}^2}\right) + \left(1 + \frac{f_\pi^2}{f_{\pi/2}^2}\right)\left(1 - \frac{f_0^2}{f_{\pi/2}^2}\right) + 4\frac{f_{\pi/4}^2 f_{3\pi/4}^2}{f_{\pi/2}^4} \tag{3.74}$$

$$C = \left(1 - \frac{f_0^2}{f_{\pi/2}^2}\right)\left(1 - \frac{f_\pi^2}{f_{\pi/2}^2}\right) + 2 - 2\frac{f_{\pi/4}^2 f_{3\pi/4}^2}{f_{\pi/2}^4} \tag{3.75}$$

k_2 can then be used solve for the coupling between c-cells (k_3) using Eq. (3.76), where α is given by Eq. (3.77) and β is given by Eq. (3.78).

$$\boxed{k_3 = \frac{\beta - \alpha + k_2(1 + \alpha - \beta)}{1 - \beta(k_2 + 1)}} \tag{3.76}$$

$$\alpha = \frac{1}{f_{\pi/2}^2}\left(f_0^2 + f_\pi^2\right) \tag{3.77}$$

$$\beta = \frac{1}{f_{\pi/2}^2}\left(f_{\pi/4}^2 + f_{3\pi/4}^2\right) \tag{3.78}$$

f_1 and f_2 can then be solved for using k_2.

$$\boxed{f_1 = f_{\pi/2} \Big/ \sqrt{1-k_2}} \tag{3.79}$$

$$\boxed{f_2 = \sqrt{f_{\pi/4}^2 + f_{3\pi/4}^2 - f_1^2}} \tag{3.80}$$

And lastly f_1 and f_2 are used to solve for the coupling between a-cells and c-cells (k_1).

$$\boxed{k_1 = \sqrt{2 - 2\frac{f_{\pi/4}^2 f_{3\pi/4}^2}{f_1^2 f_2^2}}} \tag{3.81}$$

These equations are very helpful for determining if the stopband has been closed in a segment of capacitively coupled biperiodic cavities. The stopband is given by Eq. (3.82).

$$\text{stopband} = f_2\sqrt{1-k_3} - f_{\pi/2} \tag{3.82}$$

These equations are verified in the next section with measured data.

4 Measured 5-mode data

It's known that the biperiodic inductively coupled dispersion equation provides good agreement with measured normal modes in biperiodic standing wave structures [Kap 68]. However, the biperiodic capacitively coupled equation (3.64) is, to my knowledge new and still needs to be verified. To that end, the 9 normal modes of an unturned section of a biperiodic capacitively coupled x-band accelerator were measured and compared to equation (3.64).

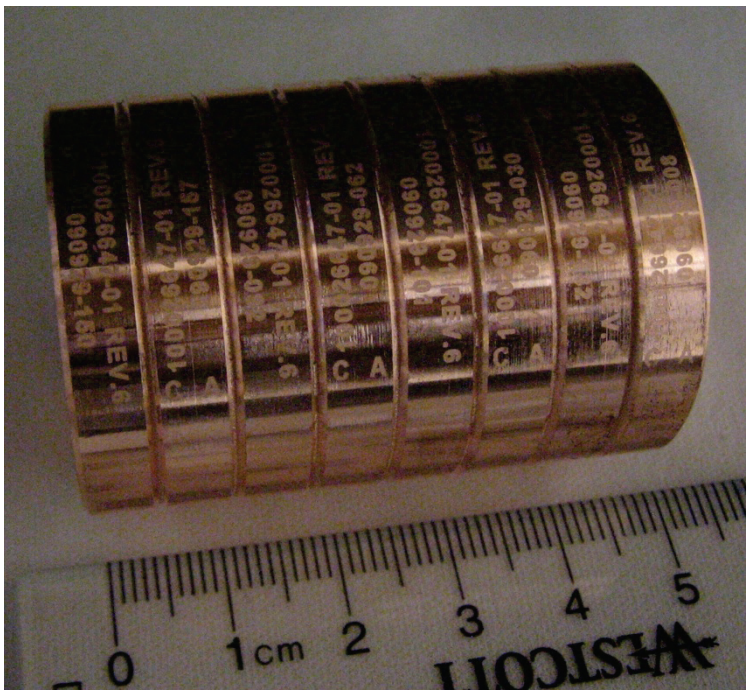

Figure 4-1: Shown is a segment of a x-band, capacitively coupled, biperiodic, standing wave accelerator used to validate the dispersion relationship obtained through the capacitively coupled equivalent circuit model.

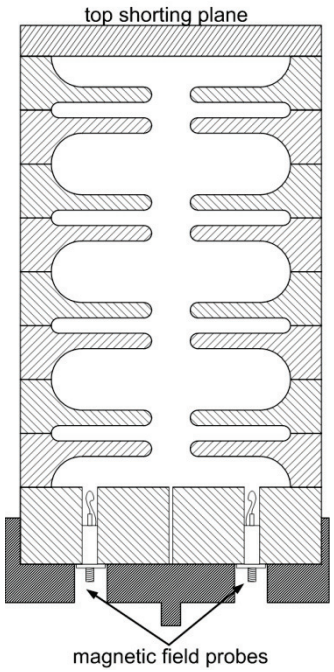

Figure 4-2: Depiction of test set up used to measure normal mode frequencies listed in Table 1

An Agilent N5230A PNA-L was employed to measure the power transmitted from one magnetic field probe to the other as a function of frequency. The peaks in the resulting spectrum are the result of the structure filling with microwave power at the structures normal mode frequencies. Special care must be taken when designing the end plate,

which will house the magnetic field probes such that the mode being measured isn't perturbed. By cleverly choosing the location of the holes it is possible reduce the capacitance and inductance of a given cavity for the TM_{101} mode equally, thus not changing the resonant frequency.

Table 1: Measured normal frequencies of the resonant structure shown in Fig. (4-2).

Mode Phase Advance [deg]	Mode frequency [MHz]
0	9192.81
22.5	9204.08
45	9232.87
67.5	9271.29
90	9300.43
112.5	9350.12
135	9374.26
157.5	9389.12
180	9394.92

Table 2: Dispersion parameters obtained using equations (3.72) through (3.81) and the data in Table 1.

k_1	0.0213
k_2	0.0029
k_3	-0.0070
f_1	9313.96 MHz
f_2	9293.69 MHz
a-cell	9300.43 MHz
c-cell	9326.29 MHz
stopband	25.86 MHz

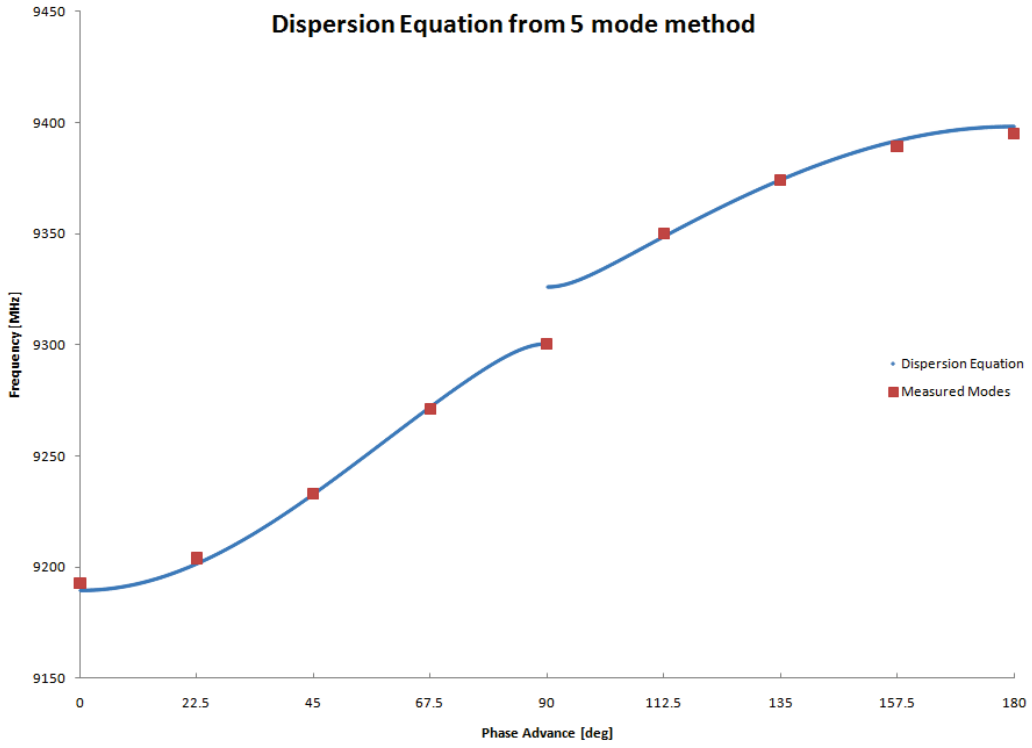

Figure 4-3: The blue curve is equation (3.64) plotted using the parameters in Table 2. The red squares are the measured modes listed in Table 1. The capacitively coupled dispersion equation shows good agreement even with a modest stopband of about +26MHz.

5 Equivalent Circuit with Losses and Dissimilar Parts.

As useful as the dispersion equations in chapter 3 are, they are limited by the fact that they assume cavities are lossless, and that the structure contains no dissimilar parts. In practice, industrial and medical accelerators do have dissimilar parts. In general these accelerators are made of buncher cavities, some type of periodic cavity, coupler cavities, and end cells. Buncher sections typically have cavities which are shorter than periodic cavities with respect to the beam line. They may also have different cell to cell coupling in order to produce a desirable field step. Coupling cavities have an iris which allows RF power to flow from the waveguide into the accelerating structure. Even the periodic cavities, which are machined as identical as possible, can have differences. These differences in dimensions between cavities cause tuning errors. Schemes can and have been devised for correcting these types of frequency errors by mechanically deforming (tuning) problem cavities as a final manufacturing step. However, understanding how dissimilar parts effect the structure's operating mode allows one to develop new tuning schemes or to design untuned accelerating structures with acceptable tolerances.

This chapter details how to include losses and dissimilar parts into the equivalent circuit model using numerical analysis techniques. This numerical model will illustrate how various types of tuning errors affect a structure's field profile. This problem will require solving a system of N coupled nonlinear differential equations, where N is the number of cavities in the structure. Calculating a system of coupled oscillator's normal modes is a familiar problem for students of classical mechanics [Tay 05], or mathematics [Edw 00]. Solving these problems usually amounts to describing the systems, and solving for the

possible eigenvectors, which satisfy an assumed solution and a given set of boundary value conditions.

5.1 3 cavity problem

As an example, let's use a circuit equivalent model of three cavities which exhibited both nearest neighbor coupling, and next nearest neighbor coupling. The goal will be to solve for the steady state current of each cavity. The inductively coupled circuit will be solved side by side with the capacitively coupled circuit.

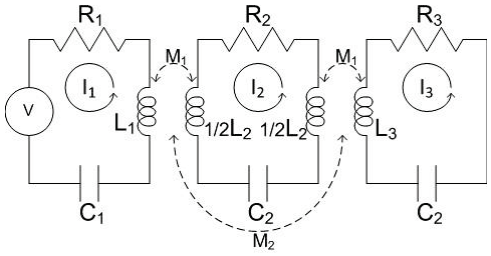

Figure 5-1: Inductively coupled three cavity circuit equivalent model.

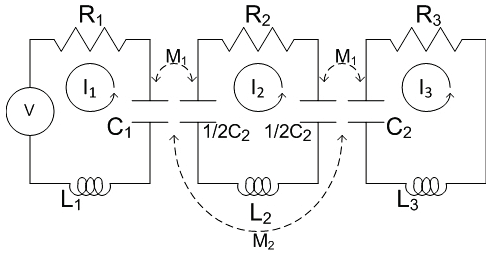

Figure 5-2: Capacitively coupled three cavity circuit equivalent model.

Using Kirchhoff's loops in the same manner as in chapter 3.

$$V = i_1\left(R_1 + \frac{1}{sC_1} + sL_1\right) + i_2 sM_1L_1 + i_3 sM_2L_1$$

$$0 = i_2\left(R_2 + \frac{1}{sC_2} + sL_2\right) + i_1 sM_1L_2 + i_3 sM_1L_2$$

$$0 = i_3\left(R_3 + \frac{1}{sC_3} + sL_3\right) + i_2 sM_1L_3 + i_1 sM_2L_3$$

$$V = i_1\left(R_1 + \frac{1}{sC_1} + sL_1\right) + \frac{i_2M_1}{sC_1} + \frac{i_3M_2}{sC_1}$$

$$0 = i_2\left(R_2 + \frac{1}{sC_2} + sL_2\right) + \frac{i_1M_1}{sC_2} + \frac{i_3M_1}{sC_2}$$

$$0 = i_3\left(R_3 + \frac{1}{sC_3} + sL_3\right) + \frac{i_2M_1}{sC_3} + \frac{i_1M_2}{sC_3}$$

Since we are interested in the steady state solution we let $s = j\omega$. Again, following the approach described in chapter 3, the tank circuit equations are used. This time however the structure is not assumed to be periodic or biperiodic.

Inductive

$$\frac{V}{L_1} = i_1\left(\frac{\omega_1}{Q_1} - j\left(\frac{\omega_1^2-\omega^2}{\omega}\right)\right) + i_2 j\omega M_1 + i_3 j\omega M_2$$

$$0 = i_2\left(\frac{\omega_2}{Q_2} - j\left(\frac{\omega_2^2-\omega^2}{\omega}\right)\right) + i_1 j\omega M_1 + i_3 j\omega M_1$$

$$0 = i_3\left(\frac{\omega_3}{Q_3} - j\left(\frac{\omega_3^2-\omega^2}{\omega}\right)\right) + i_2 j\omega M_1 + i_1 j\omega M_2$$

Capacitive

$$\frac{V}{L_1} = i_1\left(\frac{\omega_1}{Q_1} - j\left(\frac{\omega_1^2-\omega^2}{\omega}\right)\right) - i_2 j\frac{\omega_1^2}{\omega}M_1 - i_3 j\frac{\omega_1^2}{\omega}M_2$$

$$0 = i_2\left(\frac{\omega_2}{Q_2} - j\left(\frac{\omega_2^2-\omega^2}{\omega}\right)\right) - i_1 j\frac{\omega_2^2}{\omega}M_1 - i_3 j\frac{\omega_2^2}{\omega}M_1$$

$$0 = i_3\left(\frac{\omega_3}{Q_3} - j\left(\frac{\omega_3^2-\omega^2}{\omega}\right)\right) - i_2 j\frac{\omega_3^2}{\omega}M_1 - i_1 j\frac{\omega_3^2}{\omega}M_2$$

All terms are now only reference cavity parameters, except that the drive term is being divided by the coupling cavity's inductance. This is acceptable because our interests are in the phase and amplitude of the individual cavity's current with respect to each other. The drive term will affect the magnitude of each cavity's current equally, leaving the normalized peak current in each cavity unchanged. These three equations can now be written as a matrix equation in an Ohms law like form, where the product of an impedance matrix and a current matrix equals a voltage matrix.

(5.1)

$$\begin{pmatrix} \frac{\omega_1}{Q_1} - j\left(\frac{\omega_1^2-\omega^2}{\omega}\right) & j\omega M_1 & j\omega M_2 \\ j\omega M_1 & \frac{\omega_2}{Q_2} - j\left(\frac{\omega_2^2-\omega^2}{\omega}\right) & j\omega M_1 \\ j\omega M_2 & j\omega M_1 & \frac{\omega_3}{Q_3} - j\left(\frac{\omega_3^2-\omega^2}{\omega}\right) \end{pmatrix} \cdot \begin{pmatrix} i_1 \\ i_2 \\ i_3 \end{pmatrix} = \begin{pmatrix} \frac{V}{L_1} \\ 0 \\ 0 \end{pmatrix}$$

(5.2)

$$\begin{pmatrix} \frac{\omega_1}{Q_1} - j\left(\frac{\omega_1^2-\omega^2}{\omega}\right) & -j\frac{\omega_1^2}{\omega}M_1 & -j\frac{\omega_1^2}{\omega}M_2 \\ -j\frac{\omega_2^2}{\omega}M_1 & \frac{\omega_2}{Q_2} - j\left(\frac{\omega_2^2-\omega^2}{\omega}\right) & -j\frac{\omega_2^2}{\omega}M_1 \\ -j\frac{\omega_3^2}{\omega}M_2 & -j\frac{\omega_3^2}{\omega}M_1 & \frac{\omega_3}{Q_3} - j\left(\frac{\omega_3^2-\omega^2}{\omega}\right) \end{pmatrix} \cdot \begin{pmatrix} i_1 \\ i_2 \\ i_3 \end{pmatrix} = \begin{pmatrix} \frac{V}{L_1} \\ 0 \\ 0 \end{pmatrix}$$

Now to solve for the individual cavity currents, the 3 by 3 impedance matrix is inverted and multiplied by the drive term (voltage) matrix.

(5.3)

$$\begin{pmatrix} \frac{\omega_1}{Q_1} - j\left(\frac{\omega_1^2-\omega^2}{\omega}\right) & j\omega M_1 & j\omega M_2 \\ j\omega M_1 & \frac{\omega_2}{Q_2} - j\left(\frac{\omega_2^2-\omega^2}{\omega}\right) & j\omega M_1 \\ j\omega M_2 & j\omega M_1 & \frac{\omega_3}{Q_3} - j\left(\frac{\omega_3^2-\omega^2}{\omega}\right) \end{pmatrix}^{-1} \cdot \begin{pmatrix} \frac{V}{L_1} \\ 0 \\ 0 \end{pmatrix} = \begin{pmatrix} i_1 \\ i_2 \\ i_3 \end{pmatrix}$$

(5.4)

$$\begin{pmatrix} \frac{\omega_1}{Q_1} - j\left(\frac{\omega_1^2-\omega^2}{\omega}\right) & -j\frac{\omega_1^2}{\omega}M_1 & -j\frac{\omega_1^2}{\omega}M_2 \\ -j\frac{\omega_2^2}{\omega}M_1 & \frac{\omega_2}{Q_2} - j\left(\frac{\omega_2^2-\omega^2}{\omega}\right) & -j\frac{\omega_2^2}{\omega}M_1 \\ -j\frac{\omega_3^2}{\omega}M_2 & -j\frac{\omega_3^2}{\omega}M_1 & \frac{\omega_3}{Q_3} - j\left(\frac{\omega_3^2-\omega^2}{\omega}\right) \end{pmatrix}^{-1} \cdot \begin{pmatrix} \frac{V}{L_1} \\ 0 \\ 0 \end{pmatrix} = \begin{pmatrix} i_1 \\ i_2 \\ i_3 \end{pmatrix}$$

Numerical decomposition techniques can be employed to invert the impedance matrix and solve for each cavities current as a function of frequency. This technique is described in section 5.3 and shown in Appendix A.

5.2 N cavity problem

It is desirable to solve this coupled cavity problem for an arbitrary number of cavities, so that this work can be applied to numerous different efforts. Eqs. (5.3) and (5.4) are useful for showing patterns that can be used to solve the *N* cavity problem, where *N* is number of coupled cavities in a given system. The impedance matrix's dimensions in this case are *N* by *N*. The main diagonal is the same for both an inductive and capacitively coupled structure. Each element in the main diagonal has a value given by Eq.(5.5).

$$\frac{\omega_i}{Q_i} - j\left(\frac{\omega_i^2 - \omega^2}{\omega}\right) \tag{5.5}$$

The subscript i in Eq. (5.5) has a range of $1 \le i \ge N$, and it references which cavity a given property applies to. All other non-zero elements in the impedance matrix are coupling terms. These coupling terms values differ slightly between the capacitively coupled model and the inductively coupled model. The inductive coupling term is shown by Eq. (5.6) and the capacitive coupling term is shown by Eq. (5.7). Remember that $M = k/2$ can be used if the Los Alamos coupling notation is preferred. This is explained in Section 3.1.

(inductive) $$j\omega M \tag{5.6}$$

(capacitive) $$-\frac{j\omega_i^2 M}{\omega} \tag{5.7}$$

The elements in the diagonals adjacent to the right and left of the main diagonal describe the systems nearest neighbor coupling. The elements in the diagonals adjacent to the nearest neighbor coupling diagonal describe the systems next nearest neighbor coupling. And similarly, the elements in the diagonals adjacent to the next nearest neighbor coupling diagonal describe the systems next next nearest neighbor coupling. I use M_1, M_2,

and M_3 to represent nearest neighbor, next nearest neighbor, and next next nearest neighbor coupling, respectively. The ω_i term in Eq. (5.7) references the cavity who's impedance is being "seen" by the neighboring cavities, consequently the subscript i is equal to the row number the coupling term is in, within the impedance matrix.

Larger systems models will have a sparsely populated impedance matrix. Besides the main diagonal and two other minor diagonals for each level coupling being included, all other elements will be zero. So models including nearest neighbor coupling will have 3 non-zero diagonals, models including next nearest neighbor coupling will have 5 non-zero diagonals, etc.

The voltage matrix will be an N by 1 matrix with all 0 elements except in the rows corresponding to driven cavities. For example, since the first cavity is driven in Figs. (5-1) and (5-2), the element in the first row of the voltage matrix in Eqs. (5.1) and (5.2) are non zero.

The current matrix will be an N by 1 matrix, which holds the fields in each cavity when the system is driven at a steady frequency ω. The next section describes a C++ computer code which was written to solve this coupled cavity problem.

5.3 "equivalent" code description

"Equivalent" is a win32 C++ consol code, which was written to solve for the steady state currents of every cavity in a chain of N coupled cavities using the equivalent circuit model described in the previous section. Almost the entire code has been included in Appendix A. The purpose of this section is to give a brief description of what the code does with a little explanation of how it does it. In this explanation I'll point out the code line numbers using apostrophes, for example (line number).

The program reads its input variables from an input file. An example of this input file is shown in Appendix C. The first thing the program reads is the number of cavities (36), this allows the program to know how to size every vector container in the code. The program then reads in the start frequency (59), the stop frequency(63), and the number of points used to discretize the frequency space (67).

The program then reads in the voltage matrix or drive terms (84-97). Any non-zero value is equivalent to the corresponding cavity being driven. The structure being modeled with the input file shown in appendix C is driven by the 13^{th} cavity. The magnitude of this variable is arbitrary and will affect the magnitude of the current in each cavity equally.

Cavity quality factor (98-107) and cavity frequency (108-117) are read in the same fashion. In all three cases the values are held in a vector container in sequential order from first to last. Since each cavity's properties are entered into the code individually,

any coupled cavity structure can be modeled: periodic, biperiodic, tri-periodic, dissimilar parts, etc.

The nearest neighbor coupling terms are read into a similar vector, M1[i] (118-130). Again the vector is sequential, with the first number being the coupling between cavity 1 and cavity 2, and the last number being the coupling between the second to last and last cavity. Since each coupling terms is entered separately, dissimilar coupling can be modeled as well. The next nearest neighbor coupling, M2[i], is read in to the program (131-143) in sequential order, with the first number being the coupling between cavity 1 and cavity 3, the second number being the coupling between the cavity 2 and cavity 4, etc. Next, next nearest neighbor coupling, M3[i], is read into the program (144-156) in the same fashion as M1[i] and M2[i]. All the work in this thesis sets all the M3[i] values to zero, but I programmed them in for future work.

The "cavity to be plotted" variable allows the user to pick any cavity's current spectrum to be plotted (157-176). The plot will come out as a post script file, and will plot the log of the modulus of the selected cavity's current (421-456) as a function of frequency.

The coupling type is read into program (177-182) and controls how the impedance matrix is calculated. If inductive coupling is selected, then the coupling terms are calculated using Eq. (5.6). If capacitive coupling is selected, then the coupling terms are calculated using Eq.(5.7).

The last option on the input file is to select if the simulated beadpull function should be run (188-192). This function is explained in the next section.

Once all the input information has been read into the program, the program starts solving for each cavity's complex current at every frequency specified by the input file (219). Each frequency will have a different impedance matrix, so this matrix has to built and inverted at every frequency. The impedance matrix is built using a case structure. Case 1 (222-289) is used for inductively coupled models, and case 2 (290-363) is used for capacitively coupled models. Both cases use Eq. (5.5) for the main diagonal. The values for every element in the impedance matrix are initially held in "M_con" (81) which is a vector filled with object of the complex class. "M_con" is passed into the object "a" (371) using a call by reference, and then "a" is passed into the function "comgaussj" (373). This function is declared in the header file "comgaussj.h" which is shown in Appendix B. This is a version of the published header gaussj.h [Pre 07] which has been modified to accept objects of the type NRmatrix<complex>. "comgaussj" returns the inverse of the impedance matrix using a Gauss-Jordan elimination method with full pivoting. In the future I plan to test LU decomposition methods in effort to speed up the program. The current matrix is then obtained by taking the product of the inverted impedance matrix and the voltage matrix (375-383). These current values are logged in a comma delimited excel sheet, and in the variable "databrick", which will hold the value of every cavity's current at every frequency step. Then, the loop then steps forward one step in frequency space (397-398), and the process starts over.

After the main loop is complete, the variable “databrick” contains the steady state complex current of every cavity at every frequency value used. The “databrick” is then passed into the “mass_peak_finder” function (502-559). This function looks at the modulus of every cavity’s current and searches for peaks in that spectrum. It defines a peak as a value that is larger than its three nearest neighbors on either side in its spectrum. The peaks that are found are recorded in a comma delimited excel sheet, and in a variable named “peakbrick”.

5.4 "Equivalent" code simulated beadpull

This section of code (457-475) can be ignored or activated by entering a "y" or "n" in the input file. Strictly speaking, this section of code doesn't simulate a beadpull experiment at all, since no fields are being perturbed, and no modal frequency shift is being measured. I call it a simulated beadpull because it provides the relative peak electric field values in each cavity, much like a beadpull experiment.

When this code is executed, the user is prompted to enter a frequency. The code takes this entered frequency and returns the square of the modulus of every cavity's current at the closest point to that frequency. These values are then recorded in a coma delimited text file called "beadpull.txt".

5.5 No stopband

In order to glean some understanding from the equivalent code, specific examples can be used. Fig. (5-3) shows a graphical depiction of a biperiodic x-band standing wave accelerator which was designed and built at Varian Medical Systems. This structure will be used in all the case studies in this chapter.

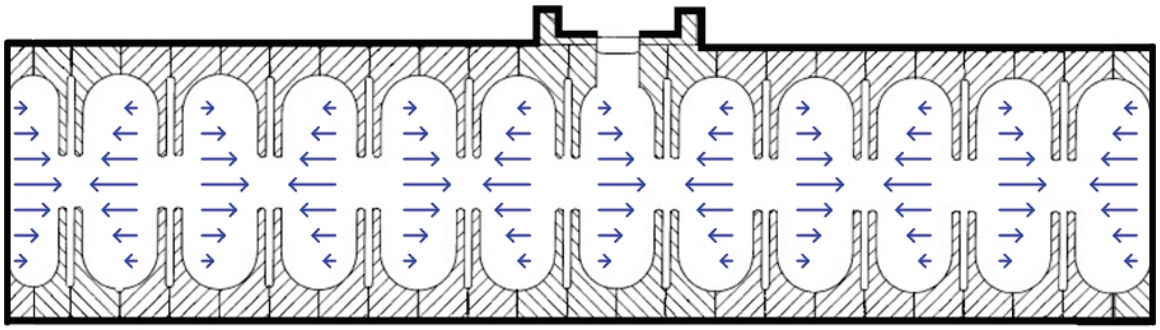

Figure 5-3: Depicted is a 23 cavity biperiodic, on axis, capacitively coupled, x-band linearly accelerator operating in the π/2's mode. Simplified electric field lines shown in blue at a phase corresponding to peak electric field.

This accelerator structure has 12 accelerating cavities (a-cells) and 11 coupling cavities (c-cells). It is coupled to waveguide through an iris in the 7^{th} a-cell. The coupling constants are shown in Table 2 and again in Table 3. These values are assumed to be constant throughout the structure. The quality factor of each cavity was set to 10,000. This value is higher than is realistic for the a-cells and certainly too high for the c-cells, but fixing the value will serve the purpose of reducing the number of variables while the affects of tuning are studied.

Since this structure is biperiodic and capacitively coupled, Eq. (3.64) was used to set f_1 (a-cell) and f_2 (c-cell) such that the stopband given by Eq.(3.65) was zero. f_1 was set equal to 9013.96 MHz since that is what was measured in chapter 4. Using these parameters,

the f_2 value which minimizes the stopband is 9267.06 MHz. These settings are shown on Table 3 with the inputs in blue boxes, and the calculated values in green boxes. Remember that f_1 and f_2 are the frequencies that the cavities would resonate at if they were by themselves, and $f_{\text{a-cell}}$ and $f_{\text{c-cell}}$ are the frequencies they resonate at now that they are coupled to other cavities. Eqs. (5.8) and (5.9) are derived from Eq. (3.64), and are used to calculate how $f_{\text{a-cell}}$ and $f_{\text{c-cell}}$ depend on f_1 and f_2. This relationship is plotted on Fig. (3-16).

$$f_{\text{a-cell}} = f_1\sqrt{1-k_2} \tag{5.8}$$

$$f_{\text{c-cell}} = f_2\sqrt{1-k_3} \tag{5.9}$$

Fig. (5-4) shows the equivalent codes simulated beadpull using the inputs described above. The equivalent code calculated the π/2 normal mode frequency to be 9301.53 MHz.

Table 3: Blue boxes show values used as inputs into the equivalent code. Green boxes show properties predicted by equation(3.64), most notably the absence of a stopband.

k_1	0.0213
k_2	0.0029
k_3	-0.007
f_1	9313.96
f_2	9268.06
$f_{\text{a-cell}}$	9300.44
$f_{\text{c-cell}}$	9300.44
Stopband	0

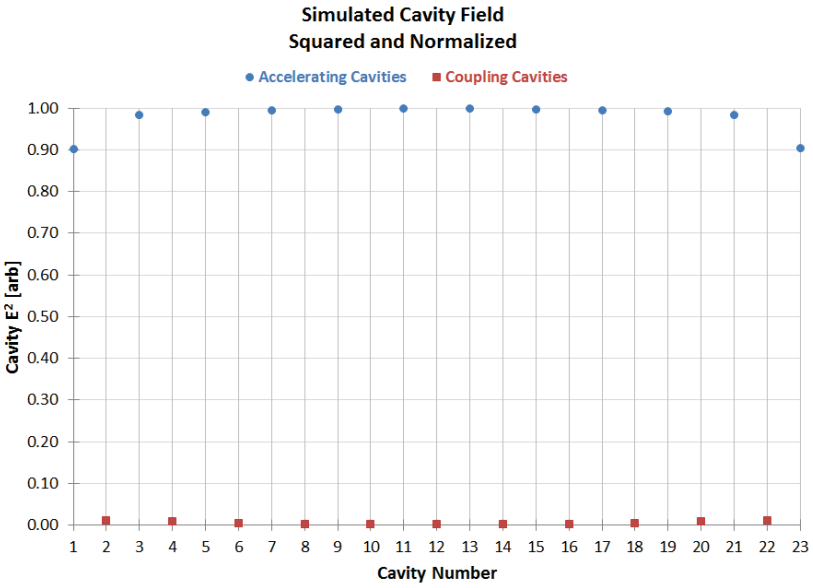

Figure 5-4: Equivalent code simulated bead pull. All E^2 values are normalized to the largest value. Structure shows moderate field steps in the accelerating cavities at the end cells. Simulated field levels taken at 9301.53MHz.

The first thing to notice about Fig.(5-4) is that field levels are, in general, just what one would expect them to be; There are nulls in the coupling cavities, and the square of accelerating cavity's electric field amplitude is relatively flat across the structure. However, the $\pi/2$ normal mode frequency is 1.09 MHz higher than Eq.(3.64) predicts, and looking closer at the field levels Fig.(5-5) does show some non-ideal behavior.

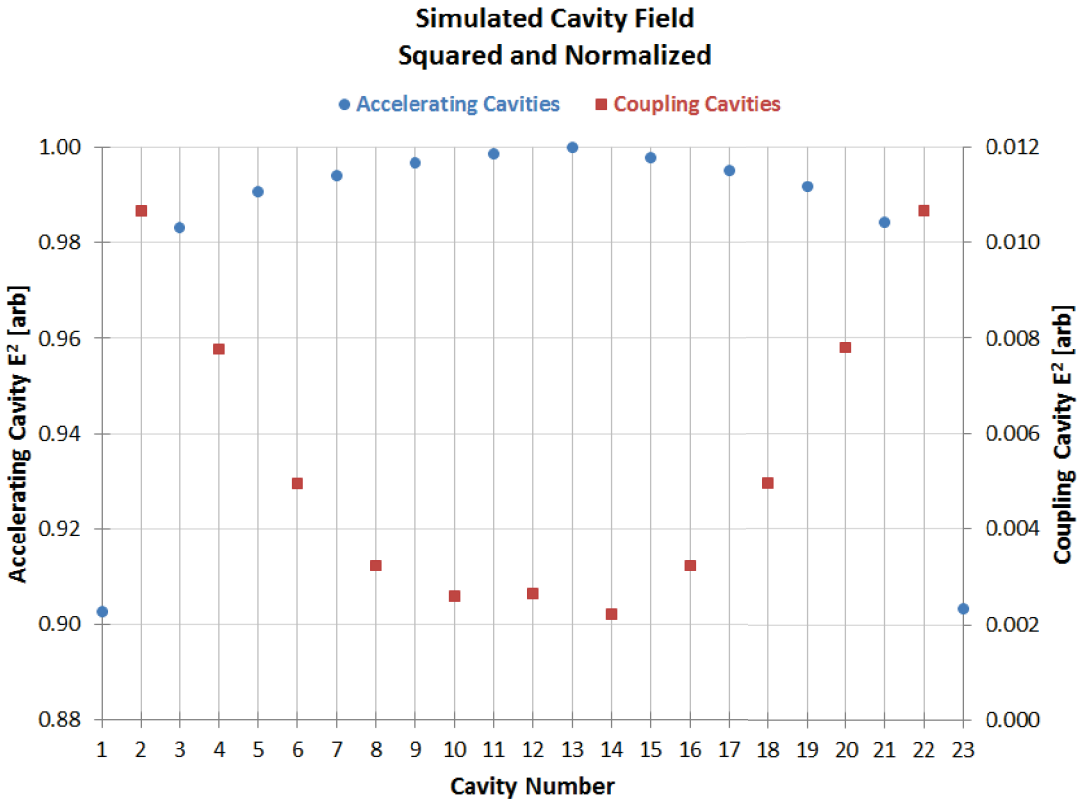

Figure 5-5: Same result shown on Fig. (5-5) except the scales on the y-axes have been adjusted to provide a magnified view.

There are two noticeable field steps at both ends of the structure. This is due to the end cells being mistuned. Unlike every other accelerating cavity in the structure, the end cells are only coupled through next nearest neighbor coupling to one other accelerating cavity. In order to compensate for this, f_1 in the end cells, needs to be adjusted. To calculate an approximate value for this end cell frequency correction, Eq. (5.10) is used with

$f_{\text{a-cell}}$ equal to (9300.44 MHz) and k_2 equal to (0.0029/2).

$$f_{\text{end}} = f_{\text{a-cell}} \Big/ \sqrt{1 - \frac{k_2}{2}} \tag{5.10}$$

When this new f_{end} value (9307.19MHz) is used at both end cells of the structure, the resulting field profile is much more ideal as shown by Fig. (5-6).

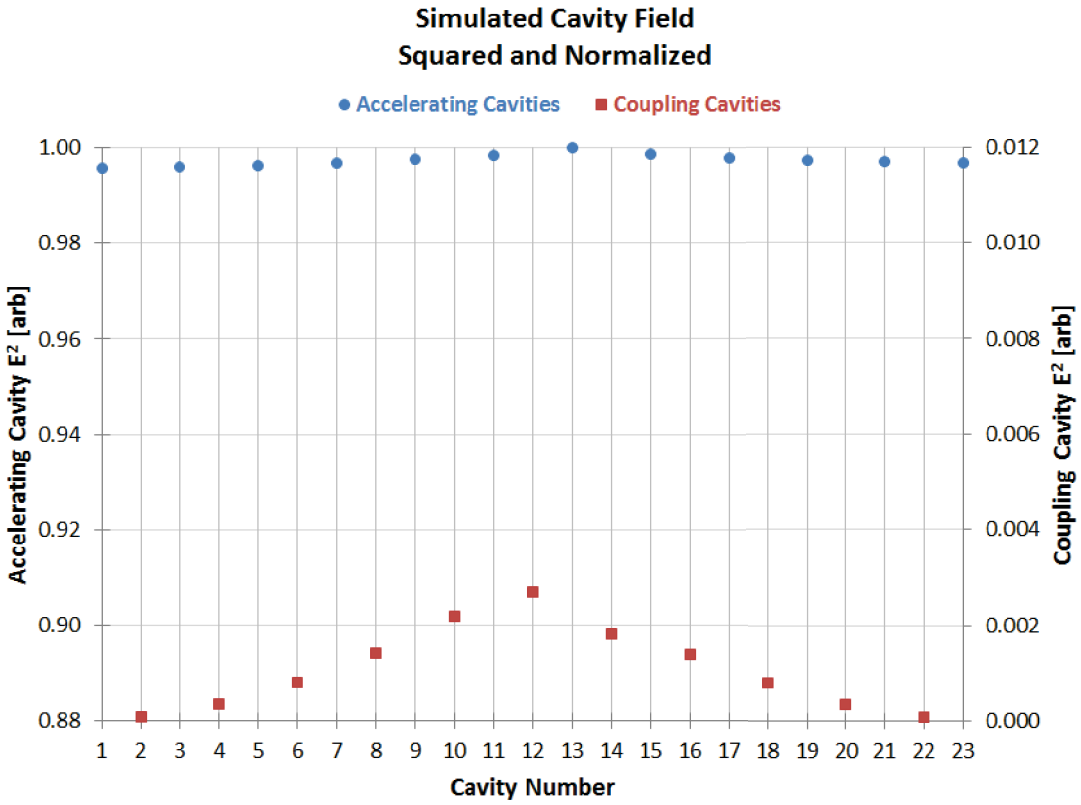

Figure 5-6: Equivalent code simulated beadpull with ideal tuning and end cell frequencies adjusted according to Eq.(5.10). Plot shows significantly more ideal field distribution compared to Fig. (5-5). Simulated field levels taken at 9300.44MHz.

With the end cell frequencies adjusted, the equivalent code now calculates the π/2's normal mode frequency at 9300.44 MHz in agreement with Eq. (3.64) as in table 3. The small amount of droop, seen in Fig. (5-6), on either side of cavity number 13 in the acceleration cavities, and cavity 12 in the coupling cavities is caused by cavity losses.

Fig. (5-7) shows the equivalent code beadpull simulation using the same parameters as those used in Fig. (5-6), except the modeled structure was made lossless.

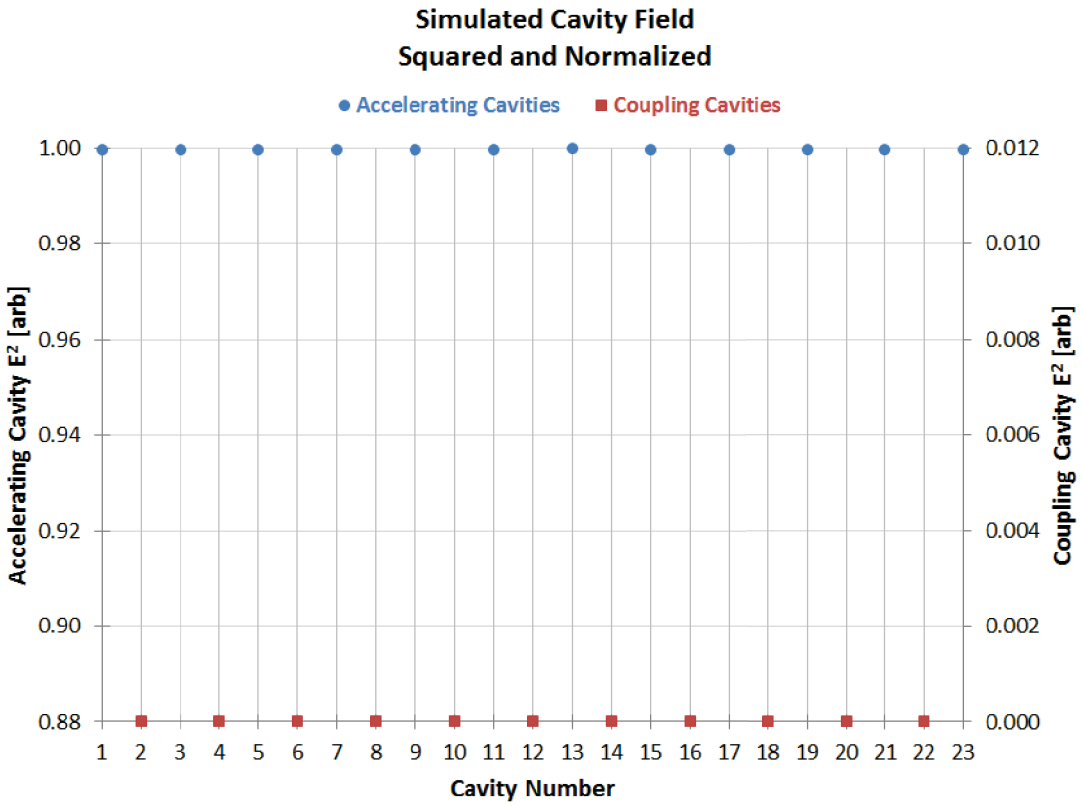

Figure 5-7: Equivalent code simulated bead pull with ideal tuning, end cell frequency adjusted, and lossless cavities. Resulting simulated field profile match the ideal the π/2's normal mode field profile. Simulated field levels taken at 9300.44MHz.

One important observation from this section is that "correct" tuning in the acceleration cavities always resulted in reduced field in the coupling cavities. In general, elevated field levels in the coupling cavities indicate tuning errors in the accelerating cavities. Fig. (5-8) takes the data from Fig. (5-7) zooms in on just the field profile of the accelerating cavities.

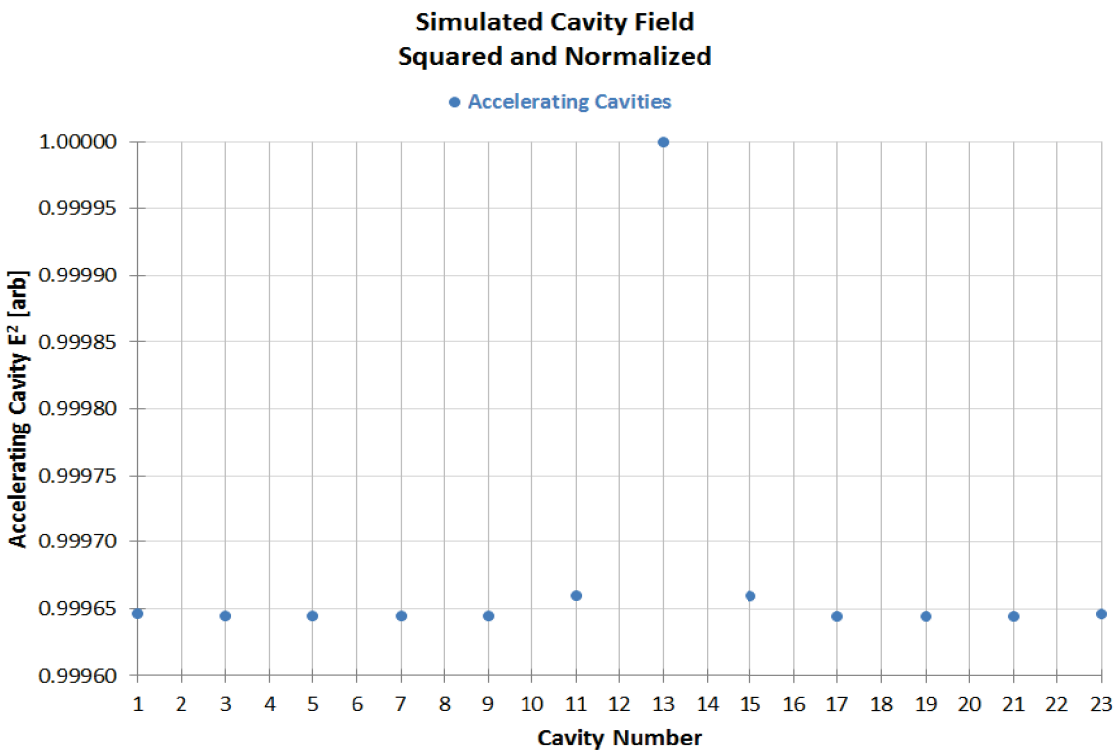

Figure 5-8: Simulated beadpull showing that there is very small effect which causes the driven cavity to be slightly mistuned by the drive term. Simulated field levels taken at 9300.44MHz.

This field "bump" at the drive cavity is very small, but present. This effect is caused by the drive term, but is not dependent on the magnitude of the drive term. I'm not sure if this is real effect or an artifact of the equivalent code. This effect could be tuned out by adjusting the f_1 value of the drive cavity. However, since the effect is so small, I'll just point it out here and then ignore it for the rest of the paper.

The reader may be wondering why the frequency in end coupling cavities were not adjusted in the same manner as the end accelerating cavities since they also experiences half of the next nearest neighbor coupling as every other coupling cavity. One expects that adjustment to be necessary; however, in all of the examples shown in this paper it had a negligible effect on the field profile.

5.6 Single a-cell tuning errors with minimal stopband

In chapter 3 we looked at two dispersion relationships of biperiodic structures. Because the structures in that chapter were considered perfectly biperiodic, those models had analytic expressions for their stopband. However, once dissimilar parts are considered, an analytic expression is not available. Despite this, it is still critical to understand how a largely biperiodic structure will behave when some of its cavities are mistuned. Chapter 6 looks at possible ways to determine stopband in a system with dissimilar parts.

Fig. (5-7) shows the ideal field distribution for a biperiodic accelerator operating in the $\pi/2$ normal mode. Figs. (5-9) and (5-10) show how this profile is perturbed when one of a-cells in the structure is mistuned. These figures were produced using the same input files as those used to produce the fields shown in Fig. (5-7), except that the 4^{th} a-cell was mistuned by +20 MHz in Fig. (5-9) and by -20 MHz in Fig. (5-10).

The field "bump" or "dip" shown in those figures is the characteristic effect of a single mistuned a-cell in a biperiodic structure with minimal stopband. I say minimal, and not zero because the one mistuned cavity is enough to produce a small stopband. The small amount of field slope seen between cavity 8 and cavity 23 is caused by this combination of the 4^{th} a-cell tuning error and a small stopband. The field slope effect is more closely looked at in the sections 5.7 and 5.8.

Table 4: Blue and red boxes show values used as inputs into the equivalent code. Green boxes show properties predicted by Eq.(3.64), most notably the absence of a stopband.

k_1	0.0213
k_2	0.0029
k_3	-0.007
f_1	9313.96
f_2	9268.06
f_{end}	9307.19
$f_{mistuned}$	9333.96
$f_{a\text{-}cell}$	9300.44
$f_{c\text{-}cell}$	9300.44
Stopband	≈0

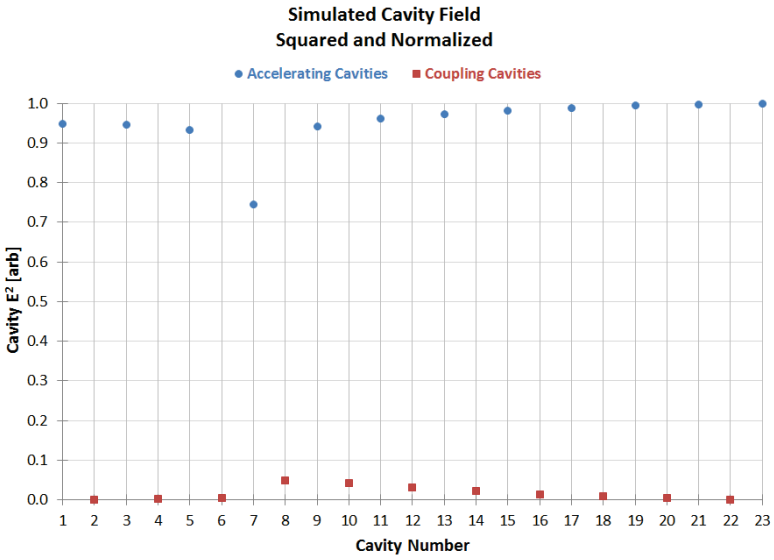

Figure 5-9: Equivalent code simulated bead pull with ideal tuning in every cavity except the 7th. The 7th cavity or the 4th accelerating cavity has been perturbed by +20MHZ. Minimal stopband in structure.

Table 5: Blue and red boxes show values used as inputs into the equivalent code. Green boxes show properties predicted by Eq.(3.64), most notably the absence of a stopband.

k_1	0.0213
k_2	0.0029
k_3	-0.007
f_1	9313.96
f_2	9268.06
f_{end}	9307.19
$f_{mistuned}$	9293.96
$f_{a\text{-}cell}$	9300.44
$f_{c\text{-}cell}$	9300.44
Stopband	≈0

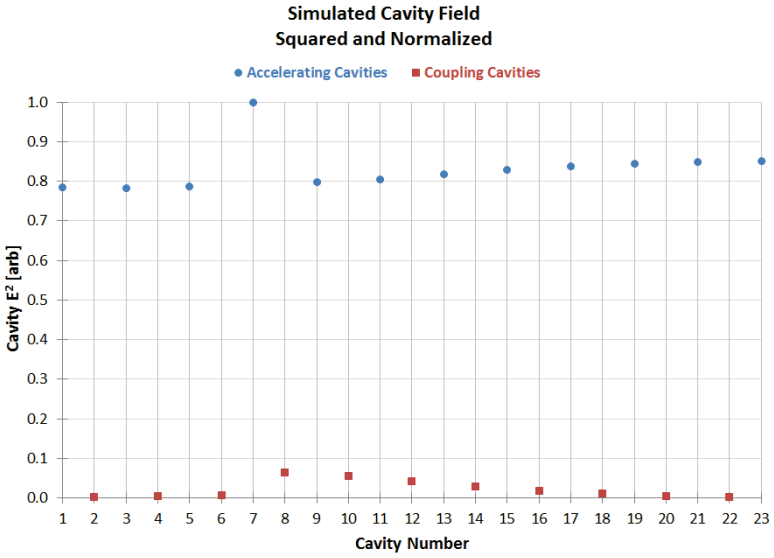

Figure 5-10: Equivalent code simulated bead pull with ideal tuning in every cavity except the 7th. The 7th cavity or the 4th accelerating cavity has been perturbed by -20MHZ. Minimal stopband in structure.

5.7 Single a-cell tuning errors with stopband

A mistuned a-cell will have a different effect from that seen in section 5.6, depending on both the magnitude and sign of the structure's stopband. Field slope is observed when a biperiodic structure has both an a-cell tuning error and a stopband. This slope increases as the tuning error in the a-cell and/or the stopband increase. The direction of the slope depends on the sign of both the tuning error in the a-cell and the stopband. If both have the same sign, the slope will be negative in the direction going outward from the mistuned a-cell. Otherwise, the slope will be positive in the direction going outward of the mistuned a-cell.

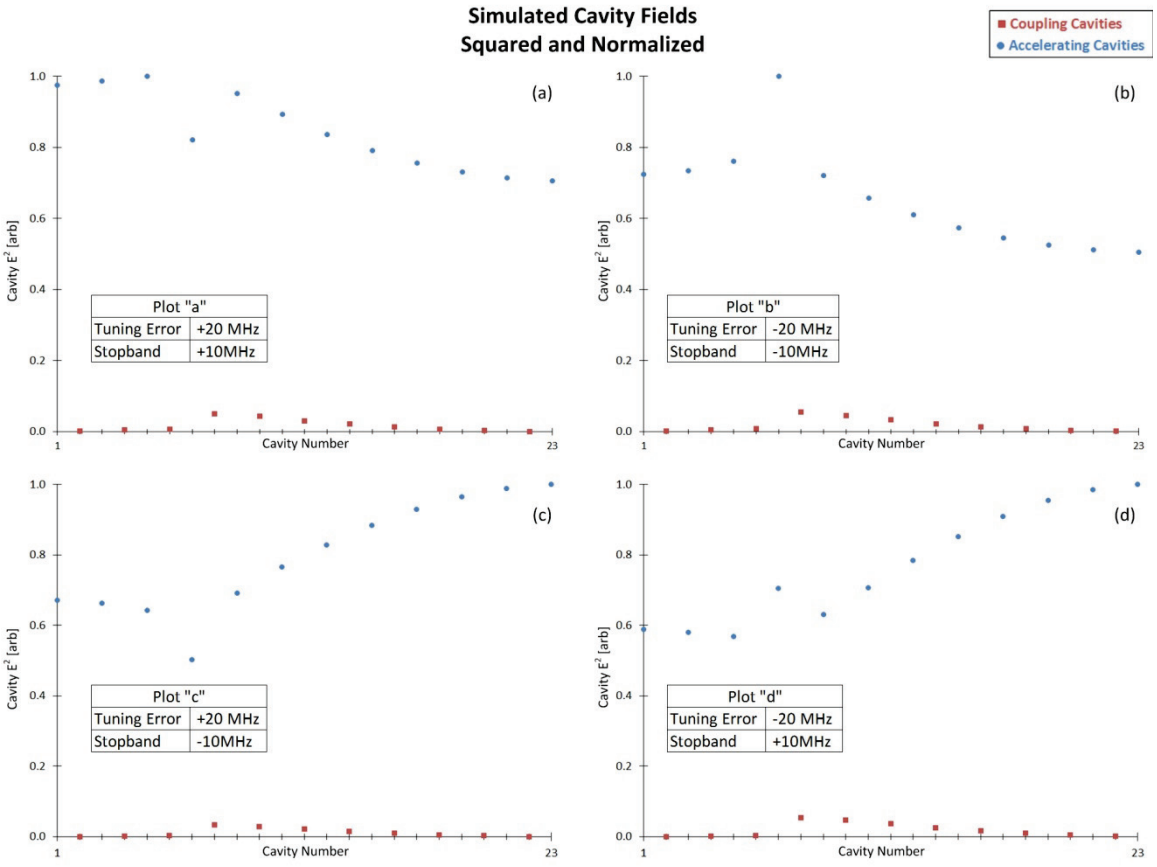

Figure 5-11: Equivalent code simulated beadpull showing field profiles with both positive and negative a-cell tuning errors in combination with positive and negative stopband.

The input file used to produce the plots in Fig. (5-11) was very similar to the ones used to make Figs. (5-9) and (5-10). The only difference was the presence of a larger stopband in Fig. (5-11). Plots in Fig (5-11) labeled as having a stopband of -10MHz had f_2 values of 9258.06MHz, and those labeled as having a stop band of +10MHz had f_2 values of 9278.06MHz.

5.8 End cell tuning errors with stopband

End cell mistuning with stopband has a very similar effect on a structure's field profile as any other mistuned a-cell with a stopband. Both produce field slope, and in both cases the direction of that slope is determined in the same way. However, in most cases shown in Fig. (5-12), when the end cells are mistuned there is a greater difference between the minimum and maximum peak cavity field throughout the structure. Practically, this means that end cell tuning errors have the potential to be more costly in standing wave accelerators similar to the one shown in Fig. (5-3).

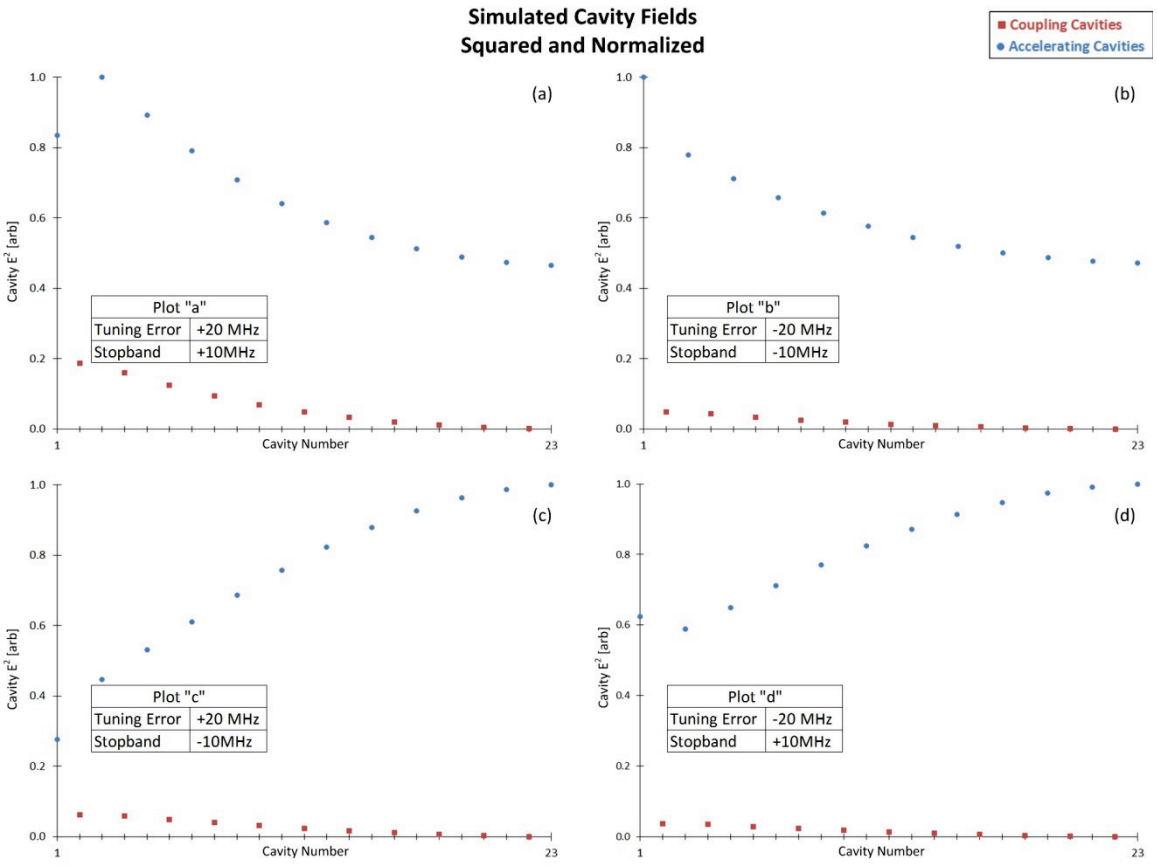

Figure 5-12: Equivalent code simulated beadpull showing field profiles with both positive and negative end cell tuning errors in combination with positive and negative stopband. As in section 5.7, the stopband was formed by changing all the f_2 values by ±10MHz.

5.9 Single c-cell tuning errors

A single mistuned coupling cavity has surprisingly little effect on a structures field profile, if all other cavities are tuned properly. Even a tuning error as large as 50MHz has a negligible effect on this structure's field profile.

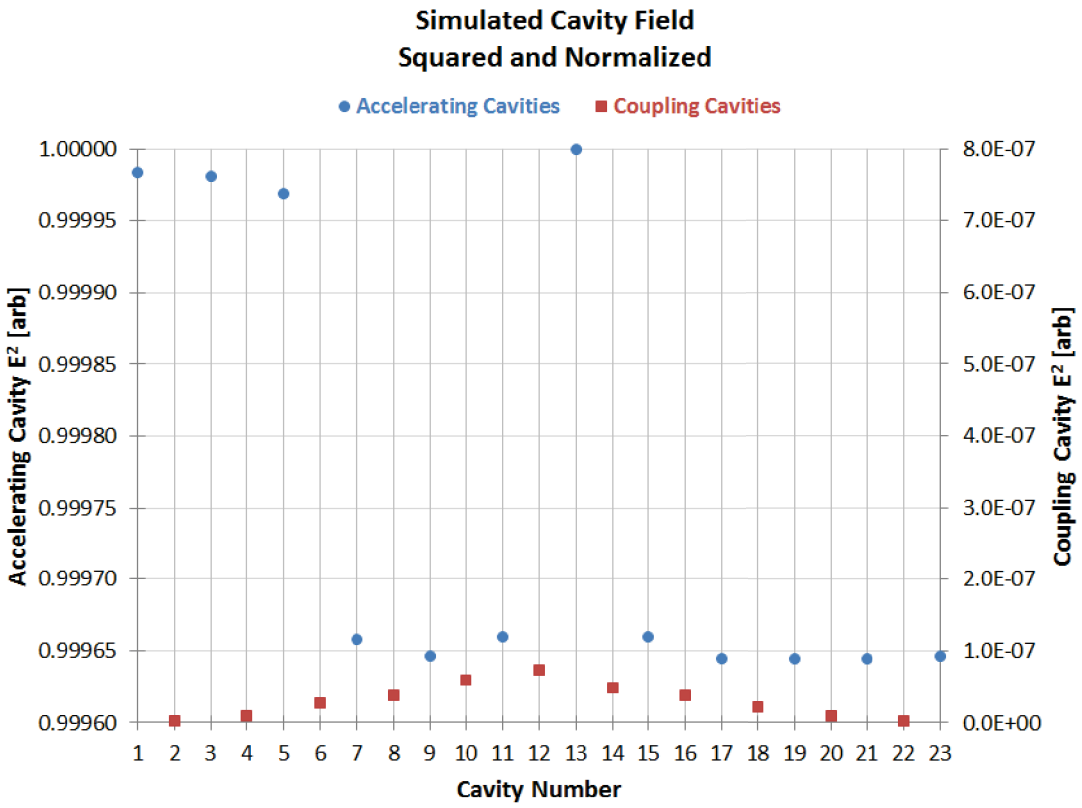

5-13: Cavity 6 (3rd c-cell) is mistuned by +50MHz the rest of the structure is perfectly tuned with the exception of the coupling cavity, discussed in section 5.5. Simulated field levels taken at 9300.44MHz.

This field step between the 5th and 7th cavity is the characteristic effect of a mistuned c-cell. However, this effect is negligible if the rest of the structure is near perfectly tuned.

The field bump seen at cavity 13 is caused by the coupling cavity being slightly mistuned. This was discussed in section 5.5.

5.10 Combinations of c-cell & a-cell tuning errors

Fig. (5-14) used the same input file as Fig. (5-13) except that cavity 21 (a-cell 11) was mistuned by +10 MHz. The mistuned a-cell caused the now expected characteristic field bump, but it also increased the magnitude of the field step between cavity 5 and 7 by a factor of about 400. Note the tuning errors on opposite sides of the structure are still coupled together and there effects are interdependent.

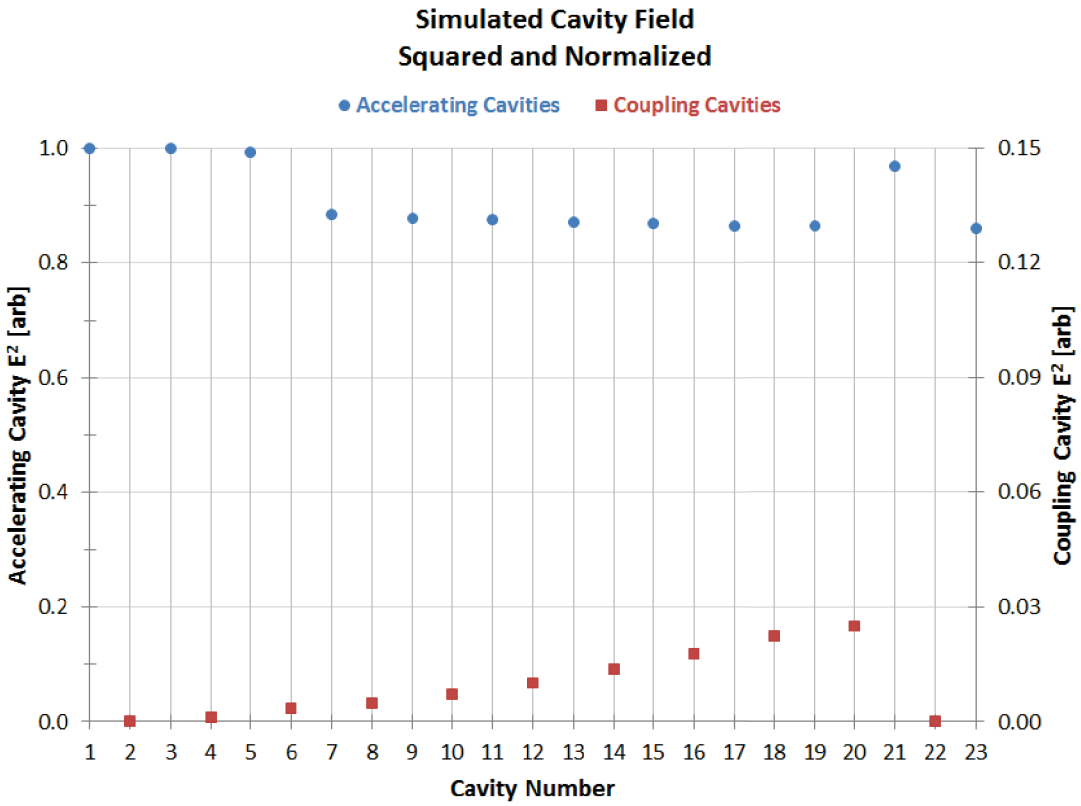

5-14: Cavity 6 (3rd c-cell) is mistuned by +50MHz, and cavity 21 (11th a-cell) is mistuned by -10 MHz. Simulated field levels taken at 9299.58 MHz.

The direction of the field step caused by the mistuned c-cell also depends on the sign of the a-cell tuning error. Fig. (5-15) illustrates. In all four cases the magnitude of the step stays the same and the field bump/dips in the 11th a-cell are all as predicted by section

5.6, but the direction of the step depended on if the c-cell and a-cell errors had the same sign or not.

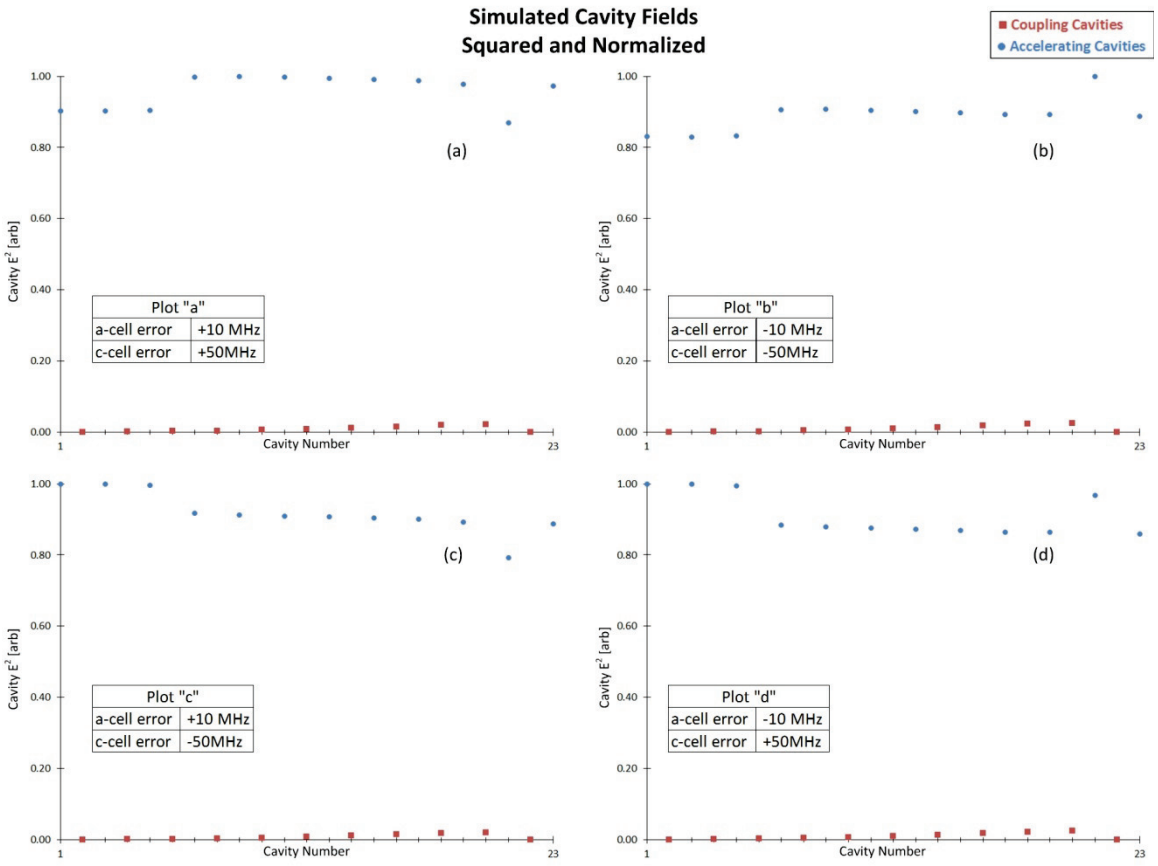

5-15: Cavity 6 (3rd c-cell) is mistuned by ±50MHz, and cavity 21 (11th a-cell) is mistuned by ±10 MHz. Plot (d) is the same as Fig. (5-14). Besides cavity tuning being changed as described above all plots use the same parameters as Fig. (5-7).

Complementary to the plots in Chapter 5 we notice that the fields in the coupling cavities increase as they approach the mistuned a-cells. Also, notice that any change that made the field in a-cells flatter (more ideal) also decreased the field in the coupling cavities. These are useful pieces of information when developing tuning protocols for biperiodic standing wave accelerators.

5.11 Coupling errors

Just as cavity tuning errors are caused by mechanical dimensional errors in high field areas of the cavities, coupling errors are caused by mechanical dimensional errors in areas where magnetic or electric fields lines move into nearby cavities. Errors that cause dissimilar coupling within the biperiodic standing wave structure have a very noticeable effect on the structures electric field profile.

If for example, a coupling slot is dissimilarly reduced in size by some factor, the first and most significant effect of that reduction will be caused by the change in nearest neighbor coupling between the two cavities on either side of the slot. Despite not directly effecting the resonant frequency of either cavity, the perturbation in nearest neighbor coupling will cause a field step; as depicted in Fig. (5-16).

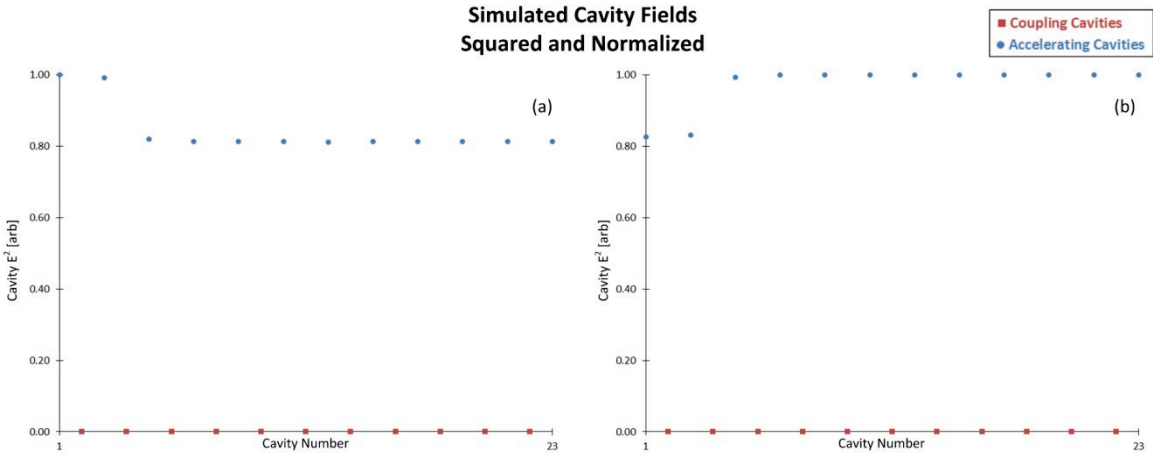

5-16: Nearest neighbor coupling was decreased by 10% in plot (a) and increased by 10% in plot (b). In both plots the coupling between the 3rd and 4th cavity was changed. Besides nearest neighbor coupling term being changed both plots use the same parameters as Fig. (5-7). Simulated field levels taken at 9300.44MHz.

The second effect will be from the next nearest neighbor coupling also being affected. Changes to next nearest neighbor coupling will cause the resonant frequency to shift in the adjacent cavities by approximately the amount predicted by Eqs. (5.8) and (5.9). The resulting frequency shifts affect the electric field profile in the manner described in sections 5.6 and 5.7.

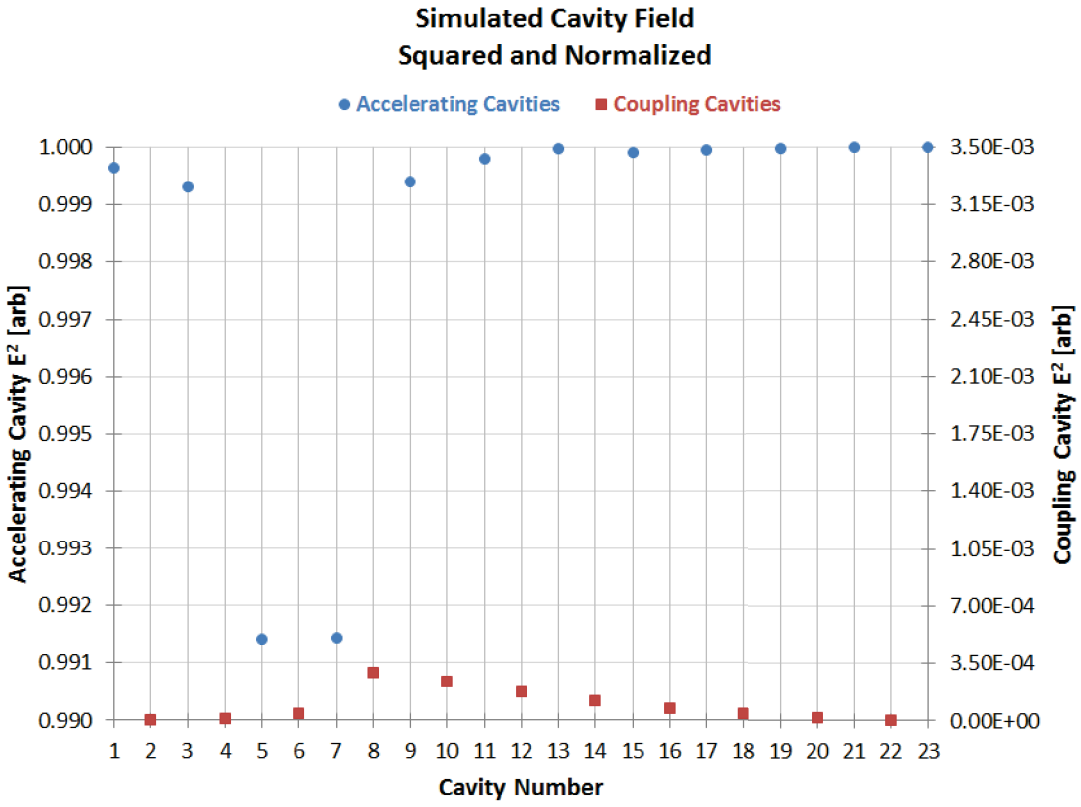

5-17: Next nearest neighbor coupling was decreased by 10% between the 3rd and 4th a-cell. This increased the frequency of the two neighboring a-cells (Eq.(5.8) and a-cells dissimilarly tuned high in frequency cause field dips. Besides next nearest neighbor coupling term being changed 5-17 uses the same parameters as Fig. (5-7). Simulated field levels taken at 9300.54 MHz (slightly higher than 5-7).

6 Measuring stopband

Field profiles are not the only way to extract useful information from the equivalent code. Since all the cavities are coupled, the current spectrum of each cavity contains information about every other cavity in the structure. Fig. (6-1) shows cavity field spectrums of both an a-cell (cavity 13) and a c-cell (cavity 12), produced by the equivalent code modeling the structure depicted in Fig. (5-3). In this simulation the a-cells were given a quality factor of 10,000 and the c-cells were given a quality factor of 5,000. The end cell f_1 values were corrected as described in section 5.5.

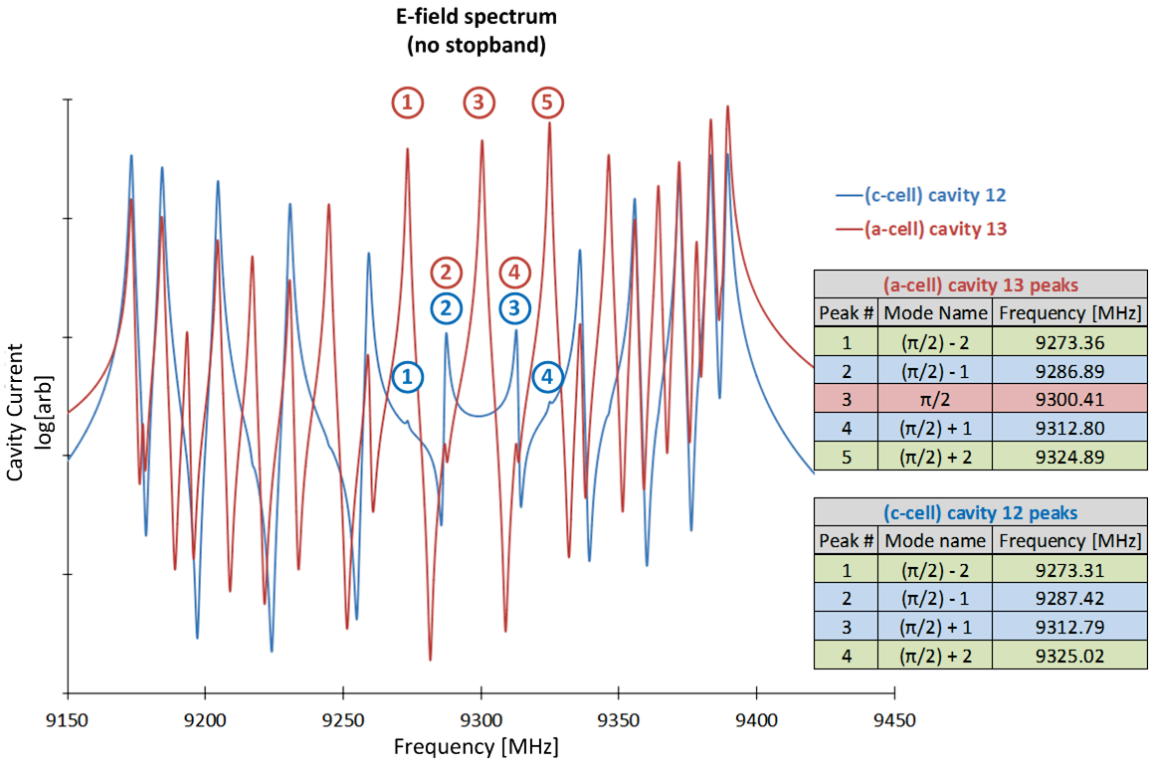

(a-cell) cavity 13 peaks		
Peak #	Mode Name	Frequency [MHz]
1	(π/2) - 2	9273.36
2	(π/2) - 1	9286.89
3	π/2	9300.41
4	(π/2) + 1	9312.80
5	(π/2) + 2	9324.89

(c-cell) cavity 12 peaks		
Peak #	Mode name	Frequency [MHz]
1	(π/2) - 2	9273.31
2	(π/2) - 1	9287.42
3	(π/2) + 1	9312.79
4	(π/2) + 2	9325.02

6-1: Simulated current spectrum of the structure depicted in Fig. (5-3). This spectrum shows the value each normal mode when the structure is perfectly tuned.

The peaks on these curves occur at the structures normal modes, and their location can be used to measure the stopband of a given structure. The catch is that the ideal mode placement must be known, and the structure cannot be too mistuned. In this case it is

known that the model structure used to produce Fig. (6-1) was perfectly tuned, so Fig. (6-1) shows the ideal location of every normal mode in the structure.

Fig. (6-2) shows how this ideal spectrum is shifted when the coupling cavities are equally mistuned producing a known stopband of -10MHz. Notice that the π/2 mode doesn't move but every other mode is shifted. The direction of the shift is given by the sign of the stopband. In this case the stopband is negative, so the spectrum is shifted down in frequency. However, if the stopband had been positive, the spectrum would have shifted up in frequency. Also, notice that the magnitude of the shift is about twice as large on the lower frequency side of the π/2 mode. Had the stopband been positive, than the shift on the higher frequency side of the π/2 mode would have been larger.

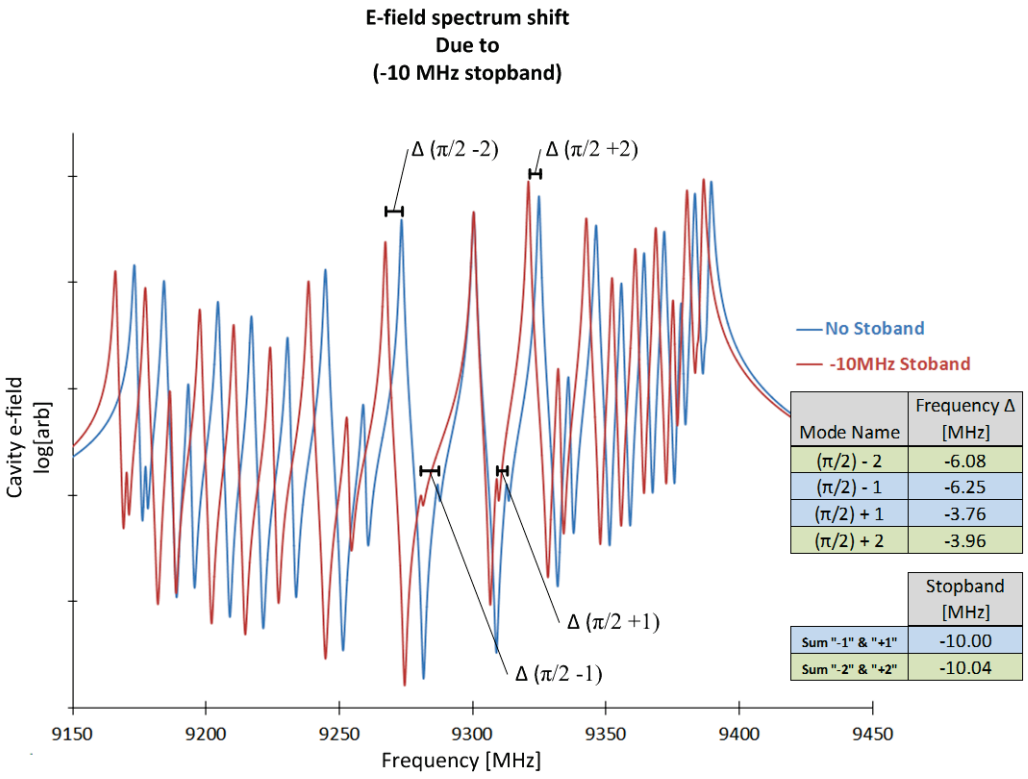

6-2: Spectrum shift caused by a uniform -10MHz tuning error in the coupling cavities. The sum of the shift in the neighboring modes yields the value of the stopband.

The sum of the frequency shift from the ideal value of normal modes of equal modal separation from the $\pi/2$ mode (i.e. the modes $\pm x$ from the $\pi/2$ mode) is equal to the structures stopband.

7 Summary

To apply the results of this thesis work to analyze a biperiodic standing wave accelerator, the first step is to determine the coupling parameters. The easiest way to do that is by using the 5-mode method described in chapter 5. These 5 modes can be obtained via microwave measurements on a portion of the structure, or using electromagnetic simulation software like Ansoft or CST Microwave Studio. Of course the equations in chapter five describe a capacitively coupled device, so if the structure is inductively coupled, the references noted in chapter 5 should be used. Once the coupling constants are known, the optimum "end cell" resonate frequencies can be determined using equation (5.10). Then the equivalent code can be used to model the structures field profile. The combination of this with a macro particle code permits one to relate industrial accelerator specs like output, spot size, and power requirements with mechanical manufacturing tolerances.

Alternatively, chapters 5 and 6 can be used more qualitatively to help diagnose the cause of a misbehaving biperiodic accelerator.

In the future one could improve on the equivalent code approach in some of the following ways. The speed of the program could be greatly improved by using more specialized algorithm to invert the impedance matrix (chapter 5.3), and rewrite the codes using Microsoft's PPL (parallel patterns library) to invert multiple impedance matrices at the same time. If sufficient speed improvement is achieved it might be possible to have the

program read in a field profile measurement, and then solve for the most likely cavity properties capable of producing that profile.

References

[Nag 67] D. Nagel, E. Knapp, B. Knapp
Coupled Resonant Model for Standing Wave Accelerator Tanks
Review of Scientific instruments Volume 38, Number 11

[Nap 68] E. Knapp, B. Knapp, J. Potter
Standing Wave high Energy Linear Accelerator Structures
Review of Scientific Instruments Volume 39, Number 7

[Kim 07] S.H. Kim, H.R. Yang, S.I. Moon, J. Jang, Y.M. Gil, M. Cho, W. Namkung
Cold Test on c-band Standing-Wave Accelerator
Proceedings of PAC07, Albuquerque, New Mexico, USA

[Jac 62] J.D Jackson
Classical Electrodynamics 2nd edition
New York: John Wiley & Sons, 1962. Print

[Pre 07] W. Press, S. Teukolsky, W Vetterling, B Flannery
Numerical Recipes, The Art of Scientific Computing 3rd edition
New York: Cambridge University Press, 2007. Print

[Edw 00] H. Edwards, D. Penney
Elementary Differential Equations with Boundary Value Problems 4th Edition
New Jersey: Prentice-Hall, 2000. Print

[Wan 98] T. Wangler
RF Linear Accelerators
New York: John Wiley & sons, 1998. Print

[Whi 98*] D. Whittum
Introduction to Microwave Linacs
SLAC-PUB-8026

[Whi 98] D. Whittum
Introduction to Electrodynamics for Microwave Linacs
SLAC-PUB-7802

[Sch 75] S. Schriber
Comparison of Standing Wave Accelerators Operating in the $2\pi/3$ *and* $\pi/2$ *Modes*
IEEE Transactions on Nuclear Science, Vol.NS-22, No.3, June 1975

[Tay 05] John Taylor
Classical Mechanics
University Science Books, 2005. Print

[Sek 85] J. Sekutowicz, S. Kuliński, M. Pacham
Frequency Dependent Capacitive – Inductive Model for Axially Coupled π/2 Standing Wave Biperiodic Structures
IEEE Transactions on Nuclear Science, Vol. NS-32, No. 5, 1985

[Sha 89] O. Shanker, P. Rai Chowdhuri, r. Verma
Coupling coefficient information from the linac-mode spectrum
Review of Scientific instruments Volume 60, Number 10, 1989

[Kul 09] S. Kulinski, E. Plawski, M. Wojciechowski
Five Cell method of Tuning Biperiodic linear Standing Wave π/2 Accelerating Structures
Proceedings of PAC09, Vancouver, BC, Canada

[Yan 10] H. Yang, S. Kim, S. Jang, S. Park, M. Cho, W. Namkung
Commissioning of c-band Standing-Wave Accelerator
Proceedings of IPAC10, Kyoto, Japan

[Bri 46] L. Brillouin
Wave Propagation in Periodic Structures
McGraw-Hill Book Company, 1946, Print

Appendix

A. "Equivalent" Code

```
#include "nr3.h"
#include "comgaussj.h"
#include "psplot.h"
#include <cmath>

using namespace std;

typedef const NRmatrix<Complex> MatComplex_I;
typedef NRmatrix<Complex> MatComplex, MatComplex_O, MatComplex_IO;

//global definitions
int num_cav, Npoints;
double f_step, f_start;

int main() {
        #define _USE_MATH_DEFINES
        int end;
        int i, j, k;
        int cav_to_plot;
        double count;
        int status = 0;
        const double PI = 3.14159265358979323846;
        char buff[256];
        complex<double> mem;
        double f_end, w_step;
        double fi, wi;
        int cavplot = 0;

//declaring functions
        double max(VecDoub test_vec);
        double min(VecDoub test_vec);
        int peak_finder(VecDoub test_y, VecDoub test_x);
        vector<vector<double>>   mass_peak_finder(int   cav_num,   vector<vector<complex<double>>>
        databrick, vector<double> f_index);

//read input file
        ifstream in;
        in.open("infile.txt");
        ofstream check_out("in_check.txt");

// reading number of cavities, defining num_acell
                in.getline(buff, 255, ':');
                in >> num_cav;
                check_out << "Number of Cavities: " << num_cav << '\n';
                cout << "number of cavities: " << num_cav << '\n';
                vector<double> f(num_cav);
                vector<double> Q(num_cav);
                vector<double> V(num_cav);
                vector<double> M1(num_cav);
                vector<double> M2(num_cav);
                vector<double> M3(num_cav);
                vector<double> coup1(num_cav);
                vector<double> coup2(num_cav);
                vector<double> coup3(num_cav);
                vector<double> w(num_cav);
                vector<double> R(num_cav + 1);
                vector<double> D(num_cav + 1);
                vector<complex<double>> I(num_cav);
```

```
52                  vector<complex<double>> drive(num_cav);
53                  vector<vector<double>>  peakbrick(num_cav,num_cav);
54                  int num_acell;
55                  num_acell = (num_cav/2)+1;
56                  cout << "number of a-cells " << num_acell << '\n';

57  // reading start frequency
58                  in.getline(buff, 255, ':');
59                  in >> f_start;
60                  check_out << "Start frequency: " << f_start << '\n' ;

61  // reading end frequency
62                  in.getline(buff, 255, ':');
63                  in >> f_end;
64                  check_out << "Stop frequency: " << f_end << '\n';

65  // reading number of points, defining w_step, f_step, M_con, databrick, and f_index
66                  in.getline(buff, 255, ':');
67                  in >> Npoints;
68                  check_out << "Number of points: " << Npoints << '\n';
69                  //checks if the end frequency is greater than the start frequency
70                  if(f_end <= f_start) {
71                          std::cout << "f_end must be larger than f_start";
72                          std::cout << '\n' <<'\n';
73                          std::cout << "enter any key to quit" << '\n';
74                          std::cin >> end;
75                          return 1;
76                  }
77                  else { w_step = 2*PI* ((f_end - f_start)/(Npoints-1));}
78                  cout << "frequency step: " << ((f_end - f_start)/(Npoints-1))*1000 << " kHz" <<
79                  '\n';
80                  f_step = (f_end - f_start) / Npoints;    //used in mass peak finder

81                  vector<complex<double>> M_con( (num_cav*num_cav));
82                  vector <vector <complex <double> > > databrick(Npoints,num_cav);
83                  vector<double> f_index(Npoints);

84  // reading V's
85                  in.getline(buff, 255, ':');
86                  for(i=0; i < num_cav; i++)
87                  { in >> V[i]; }
88                  //making the drive value complex
89                  for(i=0; i < num_cav; i++) {
90                          drive[i] = complex<double> (V[i],0);
91                  }
92                  check_out << '\n' << "Drive voltage" << '\n';
93                  for(int i=0; i < num_cav; i++) {
94                          check_out << drive[i] << "   ";
95                          if( (i+1) % 10 == 0) { check_out << '\n'; }
96                  }
97                  check_out << '\n';

98  // reading Q's
99                  in.getline(buff, 255, ':');
100                 for(i=0; i < num_cav; i++)
101                 { in >> Q[i]; }
102                 check_out << '\n' << "Cavity Q Values:" << '\n';
103                 for(int i=0; i < num_cav; i++) {
104                         check_out << Q[i] << "   ";
105                         if( (i+1) % 10 == 0) { check_out << '\n'; }
106                 }
107                 check_out << '\n';

108 // reading f's
109                 in.getline(buff, 255, ':');
110                 for(i=0; i < num_cav; i++)
111                 { in >> f[i]; }
112                 check_out << '\n' << "Frequency Values:" << '\n';
113                 for(int i=0; i < num_cav; i++) {
```

```
114                         check_out << f[i] << "   ";
115                         if( (i+1) % 10 == 0) { check_out << '\n'; }
116                 }
117                 check_out << '\n';

118     // reading M1's
119                 if( num_cav > 1) {
120                         in.getline(buff, 255, ':');
121                         for(i=0; i < num_cav-1; i++)
122                         { in >> M1[i]; }
123                 }
124                 else { in.getline(buff, 255, ':'); }
125                 check_out << '\n' << "Nearest Neighbor Coupling" << '\n';
126                 for(int i=0; i < num_cav-1; i++) {
127                         check_out << M1[i] << "   ";
128                         if( (i+1) % 10 == 0) { check_out << '\n'; }
129                 }
130                 check_out << '\n';

131     // reading M2's
132                 if( num_cav > 2) {
133                         in.getline(buff, 255, ':');
134                         for(i=0; i < num_cav-2; i++)
135                         { in >> M2[i]; }
136                 }
137                 else { in.getline(buff, 255, ':'); }
138                 check_out << '\n' << "Next Nearest Neighbor Coupling" << '\n';
139                 for(int i=0; i < num_cav-2; i++) {
140                         check_out << M2[i] << "   ";
141                         if( (i+1) % 10 == 0) { check_out << '\n'; }
142                 }
143                 check_out << '\n';

144     // reading M3's
145                 if( num_cav > 3) {
146                         in.getline(buff, 255, ':');
147                         for(i=0; i < num_cav-3; i++)
148                         { in >> M3[i]; }
149                 }
150                 else { in.getline(buff, 255, ':'); }
151                 check_out << '\n' << "Next Next Nearest Neighbor Coupling" << '\n';
152                 for(int i=0; i < num_cav-3; i++) {
153                         check_out << M3[i] << "   ";
154                         if( (i+1) % 10 == 0) { check_out << '\n'; }
155                 }
156                 check_out << '\n';

157     //reading cavity response to be plotted
158                 in.getline(buff, 255, ':');
159                 in >> cav_to_plot;
160                 check_out << '\n' << "Cavity responce to be plotted: " << cav_to_plot << '\n';
161
162                 if(cav_to_plot <= 0) {
163                         std::cout << "cavity responce to plot must be larger than 0";
164                         std::cout << '\n' <<'\n';
165                         std::cout << "enter any key to quit" << '\n';
166                         std::cin >> end;
167                         return 1;
168                 }
169                 if(cav_to_plot > num_cav){
170                         cout << "cavity responce to plot must be smaller than or equal to the
171                         number of cavities";
172                         std::cout << '\n' <<'\n';
173                         std::cout << "enter any key to quit" << '\n';
174                         std::cin >> end;
175                         return 1;
176                 }
177     //reading coupling mechanics
178                 int coupling = -999;
```

```
179                     in.getline(buff, 255, ':');
180                     in >> coupling;
181                     check_out << '\n' << "Coupling(inductive = 1 or capacitive = 2): " << coupling <<
182                     '\n';

183     //reading debug output
184                     char debug = 'Z';
185                     in.getline(buff, 255, ':');
186                     in >> debug;
187                     check_out << '\n' << "Debug Output: " << debug << '\n';

188     //bead pull test output
189                     char bead_toggle = 'Z';
190                     in.getline(buff, 255, ':');
191                     in >> bead_toggle;
192                     check_out << '\n' << "Beadpull Output: " << bead_toggle << '\n';

193     //closing input file
194     in.close();
195     check_out.close();

196     //calculate cavity angular velocities
197             for(i=0; i < num_cav; i++) {
198                     w[i] = 2 * PI * f[i];
199             }

200     //calculate R values
201             for(i=0; i < num_cav; i++) {
202                     R[i] = ( w[i] / Q[i] );
203             }

204     //calculate start annular velocity
205             wi = (f_start*2*PI);

206     //opening data stream and dumping all cavity responses into "data.csv" comma delimited.
207             ofstream out("data.csv");
208             if(!out){
209                     std::cout << "can't open data file. \n";
210                     return 1;
211             }
212             //adding lables for the data output file
213             out << "frequency[MHz],";
214             for(i=0; i < num_cav; i++) {
215             out << "LOG I" << i+1 << " [arb],";
216             }
217             out << '\n';
```

```
218    //start of main loop
219            for(count=0; count < Npoints; count++) {
220                    //fill M_con
221                    switch(coupling) {
222                    case 1: //inductive
223                            //calculate coup1
224                            if(num_cav > 1) {
225                                    for(i=0; i < num_cav; i++) {
226                                            coup1[i] = wi * M1[i];
227                                    }
228                            }
229                            //calculate coup2
230                            if(num_cav > 2) {
231                                    for(i=0; i < num_cav; i++) {
232                                            coup2[i] = wi * M2[i];
233                                    }
234                            }
235                            //calculate coup3
236                            if(num_cav > 3) {
237                                    for(i=0; i < num_cav; i++) {
238                                            coup3[i] = wi * M3[i];
239                                    }
240                            }
241                            //calculate D values
242                            for(i=0; i < num_cav; i++) {
243                                    D[i] = -1*(((pow(w[i],2)) - (pow(wi,2))) / wi);
244                            }
245                            //fill matrix with 0's
246                            for(i=0; i < num_cav*num_cav; i++) {
247                                    M_con[i] = complex<double>(0,0);
248                            }
249                            //fill in main diagonal
250                            for(i=0, j=0; j < (num_cav); i += num_cav, j++) {
251                                    M_con[i+j] = complex<double>(R[j],D[j]);
252                            }
253                            //first coup1
254                            if(num_cav > 1) {
255                                    for(i=0, j=0; j < (num_cav - 1); i += num_cav, j++) {
256                                            M_con[i+j+1] = complex<double>(0,coup1[j]);
257                                    }
258                            }
259                            //second coup1
260                            if(num_cav > 1) {
261                                    for(i=num_cav, j=0; j < (num_cav - 1); i += num_cav, j++) {
262                                            M_con[i+j] = complex<double>(0,coup1[j]);
263                                    }
264                            }
265                            //first coup2
266                            if(num_cav > 2) {
267                                    for(i=0, j=0; j < (num_cav-2); i += num_cav, j++) {
268                                            M_con[i+j+2] = complex<double>(0,coup2[j]);
269                                    }
270                            }
271                            //second coup2
272                            if(num_cav > 2) {
273                                    for(i=2*num_cav, j=0; j < (num_cav-2); i += num_cav, j++) {
274                                            M_con[i+j] = complex<double>(0,coup2[j]);
275                                    }
276                            }
277                            //first coup3
278                            if(num_cav > 3) {
279                                    for(i=0, j=0; j < (num_cav-3); i += num_cav, j++) {
280                                            M_con[i+j+3] = complex<double>(0,coup3[j]);
281                                    }
282                            }
283                            //second coup3
284                            if(num_cav > 3) {
285                                    for(i=3*num_cav, j=0; j < (num_cav-3); i += num_cav, j++) {
286                                            M_con[i+j] = complex<double>(0,coup3[j]);
```

```
287                             }
288                     }
289                     break;
290             case 2:  //conductive
291                     //calculate coup1
292                     if(num_cav > 1) {
293                             for(i=0; i < num_cav; i++) {
294                                     coup1[i] = M1[i] / wi;
295                             }
296                     }
297                     //calculate coup2
298                     if(num_cav > 2) {
299                             for(i=0; i < num_cav; i++) {
300                                     coup2[i] = M2[i] / wi;
301                             }
302                     }
303                     //calculate coup3
304                     if(num_cav > 3) {
305                             for(i=0; i < num_cav; i++) {
306                                     coup3[i] = M3[i] / wi;
307                             }
308                     }
309                     //calculate D values
310                     for(i=0; i < num_cav; i++) {
311                             D[i] = -1*(((pow(w[i],2)) - (pow(wi,2))) / wi);
312                     }
313                     //fill matrix with 0's
314                     for(i=0; i < num_cav*num_cav; i++) {
315                             M_con[i] = complex<double>(0,0);
316                     }
317                     //fill in main diagonal
318                     for(i=0, j=0; j < (num_cav); i += num_cav, j++) {
319                             M_con[i+j] = complex<double>(R[j],D[j]);
320                     }
321                     //first coup1
322                     if(num_cav > 1) {
323                             for(i=0, j=0; j < (num_cav - 1); i += num_cav, j++) {
324                                     M_con[i+j+1]    =    complex<double>(0,    (-coup1[j]    *
325                                     pow(w[j],2)) );
326                             }
327                     }
328                     //second coup1
329                     if(num_cav > 1) {
330                             for(i=num_cav, j=0; j < (num_cav - 1); i += num_cav, j++) {
331                                     M_con[i+j]    =    complex<double>(0,    (-coup1[j]    *
332                                     pow(w[j+1],2)) );
333                             }
334                     }
335                     //first coup2
336                     if(num_cav > 2) {
337                             for(i=0, j=0; j < (num_cav-2); i += num_cav, j++) {
338                                     M_con[i+j+2]    =    complex<double>(0,    (-coup2[j]    *
339                                     pow(w[j],2)) );
340                             }
341                     }
342                     //second coup2
343                     if(num_cav > 2) {
344                             for(i=2*num_cav, j=0; j < (num_cav-2); i += num_cav, j++) {
345                                     M_con[i+j]    =    complex<double>(0,    (-coup2[j]    *
346                                     pow(w[j+2],2)) );
347                             }
348                     }
```

```
349                             //first coup3
350                             if(num_cav > 3) {
351                                     for(i=0, j=0; j < (num_cav-3); i += num_cav, j++) {
352                                             M_con[i+j+3]    =    complex<double>(0,    (-coup3[j]    *
353                                             ow(w[j],2)) );
354                                     }
355                             }
356                             //second coup3
357                             if(num_cav > 3) {
358                                     for(i=3*num_cav, j=0; j < (num_cav-3); i += num_cav, j++) {
359                                             M_con[i+j]    =    complex<double>(0,    (-coup3[j]    *
360                                             pow(w[j+3],2)) );
361                                     }
362                             }
363                             break;
364                     default:
365                             cout << "ERROR in input file. 1 or 2 not entered in coupling typr";
366                             std::cout << "enter any key to quit" << '\n';
367                             std::cin >> end;
368                             return 1;
369     }

370     //define MatComplex
371             MatComplex a (num_cav, num_cav, &M_con[0]);

372     //matrix is inverted
373             comgaussj(a);
374
375     //multiply the inverted matrix by the drive vector
376             for(j=0; j < num_cav; j++) {
377                     complex<double> mem (0,0);
378                     for(i=0; i < num_cav; i++) {
379                             mem = mem + (a[j][i] * drive[i]);
380                             I[j] = mem;
381                     }
382             }

383     //calculate frequency, and output to "data.csv"
384             fi = wi / (2 * PI);
385             out << fi;
386     //output the log of the modulus of each cavities response to "data.csv"
387             for(i=0; i < num_cav; i++) {
388                     out << "," << log10(abs(I[i]));
389             }
390             out << '\n';

391     //store frequency values in "f_index"
392             f_index[count] = fi;

393     //store complex current for each cavity in "databrick"
394             for(i=0; i < num_cav; i++) {
395                     databrick[count][i] = I[i];
396             }

397     //step forward in frequency space
398             wi += w_step;

399     //display progression on the consol
400             status = 100 * (count / (Npoints-1));
401             std::cout.precision(3);
402             std::cout << "main loop % complete: " << status << '\r';

403     //end of main loop
404     }

405     //close output to "data.csv"
406     out.close();
```

```
//output "un-inverted M.txt"
if( debug=='Y' || debug=='y') {
        ofstream out2;
        out2.open("uninverted M.txt");
        for(i=0; i < (num_cav*num_cav); i++){
                out2 << M_con[i] << " ";
                if((i+1) % num_cav == 0) {
                        out2 << '\n';
                }
        }
        out2.close();
}

//find all maxima for every cavity
peakbrick = mass_peak_finder(num_cav,databrick,f_index)
//these vectors will be sent to be plotted
        VecDoub Iany1(Npoints);
        VecDoub f_plot(Npoints);
        double peak_Iany1;
        double min_Iany1;

        //cout << "creation of Iany1 initiated" << '\n';
        for(i=0; i < Npoints; i++){
                Iany1[i] = log10(abs(databrick[i][cav_to_plot-1]));
        }
        //cout << "Iany1 creation compleat" << '\n';
        for(i=0; i < Npoints; i++){
                f_plot[i] = f_index[i];
        }
        // finds the highest "y" value
        peak_Iany1 = max(Iany1);
        // find lowest "y" value
        min_Iany1 = min(Iany1);

//make plot
        char *outname = "plot1.ps";
        PSpage pg(outname);
        PSplot plot1(pg, 100.0, 550, 100.0, 550);
// axis formatting (x-min,x-max,y-min,y-man)
        plot1.setlimits(f_start, f_end, min_Iany1, peak_Iany1); //sets the axis mins and maxes
      //plot1.setfont();
        plot1.xlabel("frequency [MHz]");
        plot1.ylabel("LOG S11");
        plot1.frame(); //draws a frame around the plot
      //plot1.autoscales();  //auto scale doesn't look good with this plot
        plot1.scales( (f_end-f_start)/10, (f_end-f_start)/100, (abs(min_Iany1 - peak_Iany1))/10,
(abs(min_Iany1 - peak_Iany1))/100,2,1,1,1); //(major x-ticks, minor x-ticks, major y-ticks, minor
y-ticks, 0 means no ticks, 1 means ticks only, 2 means numbers + ticks)
        plot1.setcolor(0,50,250); // red, green, blue
        plot1.lineplot(f_plot, Iany1);
        plot1.setcolor(250,50,0);
        pg.close();
    // pg.display();   //forces the plot open
```

```
457    //created bead pull data
458            if( bead_toggle == 'y' || bead_toggle == 'Y' ) {
459                    double beadpull_f;
460                    cout << "Enter operating mode frequency [MHz]: ";
461                    cin >> beadpull_f;

462                    ofstream out4;
463                    out4.open("beadpull.txt");
464                    int k4 = 0;
465                    k4 = int ((beadpull_f - f_start) / f_step);
466                    out4 << "cavity number" << "," << "Mag" << '\n';
467                    for(i=0; i < num_cav; i++) {
468                            out4 << i+1 << "," << pow( (abs(databrick[k4][i])) , 2 )  << '\n';
469                    }
470                    out4.close();
471            }
472            cout << '\n' <<  "enter any key to quit: ";
473            cin >> end;

474            return 0;
475    }

476    //find test-vec's max value
477            double max(VecDoub test_vec)
478            {
479                    cout << "max: INITIATED";
480                    double MAX = -10000;
481                    for(int i = 0; i < Npoints; i++)
482                    {
483                            if(test_vec[i] >= MAX)
484                            {MAX = test_vec[i];}
485                    }
486                    cout << '\r' << "max: COMPLETED" << '\n';
487                    return MAX;
488            }

489    //find test-vec's min value
490            double min(VecDoub test_vec)
491            {
492                    cout << "min: INITIATED";
493                    double MIN = 10000;
494                    for(int i = 0; i <  Npoints; i++)
495                    {
496                            if(test_vec[i] <= MIN)
497                            {MIN = test_vec[i];}
498                    }
499                    cout << '\r' << "min: COMPLETED" << '\n';
500                    return MIN;
501            }
```

```
//mass peak finder
vector<vector<double>> mass_peak_finder(int cav_num, vector<vector<complex<double>>> databrick,
vector<double> f_index)
        {
                cout << '\n' <<  "mass peak finder: INITIATED";
                int Npeaks = 0;
                const double PI = 3.14159265358979323846;
                vector<vector<double>>  peakbrick(num_cav+100, num_cav);
                vector<vector<complex<double>>> normpeakbrick(num_cav+100,num_cav);
                vector<vector<complex<double>>> normdatabrick(Npoints,num_cav);
                vector<int> peaksfound(num_cav);

                //loop through all cavities
                for(int j=0; j < num_cav; j++)
                {
                        int Npeaks = 0;
                        //loop through all data
                        for(int i=0; i <  Npoints - 6; i++)
                        {
                                if( (abs(databrick[i+3][j]) > abs(databrick[i+2][j])) &&
                                (abs(databrick[i+3][j]) > abs(databrick[i+1][j])) &&
                                (abs(databrick[i+3][j]) > abs(databrick[i][j]))
                                && (abs(databrick[i+3][j]) > abs(databrick[i+4][j])) &&
                                (abs(databrick[i+3][j]) > abs(databrick[i+5][j])) &&
                                (abs(databrick[i+3][j]) > abs(databrick[i+6][j])))
                                {
                                        peakbrick[Npeaks][j] = f_index[i+3];
                                        peaksfound[j] = Npeaks;
                                        Npeaks++;
                                }
                        }
                }
                ofstream out;
                out.open("peaks.csv");
                out.precision(9);

                for (int j=0; j < num_cav; j++)
                {
                        out << "frequency cav" << j+1 << "[MHz]," << "Mag" << j+1 << "," <<
                        "phase" << j+1 << '\n';
                        for( int i=0; i < Npoints; i++)
                        {
                                if(peaksfound[j] >= i)
                                {
                                        int k = 0;
                                        //k is  the same as count in main loop.
                                        k = ceil( ((peakbrick[i][j] - f_start) / f_step) - .5);
                                        out << peakbrick[i][j] << "," << abs(databrick[k][j]) <<
                                        "," << (360 * atan2( imag(databrick[k][j]) ,
                                        real(databrick[k][j]) )) / (2*PI) << '\n';
                                }
                        }
                out << '\n';
                }

                out.close();
                cout << '\r' << "mass peak finder: COMPLETED" << '\n';
                cout << "Peaks found in cav1: " << peaksfound[0] + 1 << '\n';
                return peakbrick;
        }
```

B. Header files

nr3.h & psplot.h The contents of these two header files are published [Pre 07]. Their content and usage rights are available by purchasing a copy of the work. The equivalent code in its form shown here does require them to run.

comgaussj.h This is a version of the published header gaussj.h [Pre 07] which has been modified to accept objects of the type NRmatrix<complex>. The purpose of showing the code below is to show the changes required to make the equivalent code function. Copying this routine from this work does not excuse the reader of the requirement to purchasing [Pre 07] in order to lawfully execute the code.

```
        typedef const NRmatrix<Complex> MatComplex_I;
        typedef NRmatrix<Complex> MatComplex, MatComplex_O, MatComplex_IO;
void comgaussj(MatComplex_IO &a, MatComplex_IO &b)
{
        Int i,icol,irow,j,k,l,ll,n=a.nrows(),m=b.ncols();
        double big;
        complex<double> dum,pivinv;
        VecInt indxc(n),indxr(n),ipiv(n);
        for (j=0;j<n;j++) ipiv[j]=0;
        for (i=0;i<n;i++) {
                big=0.0;
                for (j=0;j<n;j++)
                        if (ipiv[j] != 1)
                                for (k=0;k<n;k++) {
                                        if (ipiv[k] == 0) {
                                                if (abs(a[j][k]) >= big) {
                                                        big=abs(a[j][k]);
                                                        irow=j;
                                                        icol=k;
                                                }
                                        }
                                }
                ++(ipiv[icol]);
                if (irow != icol) {
                        for (l=0;l<n;l++) SWAP(a[irow][l],a[icol][l]);
                        for (l=0;l<m;l++) SWAP(b[irow][l],b[icol][l]);
                }
                indxr[i]=irow;
                indxc[i]=icol;
                if (a[icol][icol] == 0.0) throw("gaussj: Singular Matrix");
                pivinv=1.0/a[icol][icol];
                a[icol][icol]=1.0;
                for (l=0;l<n;l++) a[icol][l] *= pivinv;
                for (l=0;l<m;l++) b[icol][l] *= pivinv;
                for (ll=0;ll<n;ll++)
                        if (ll != icol) {
                                dum=a[ll][icol];
                                a[ll][icol]=0.0;
                                for (l=0;l<n;l++) a[ll][l] -= a[icol][l]*dum;
                                for (l=0;l<m;l++) b[ll][l] -= b[icol][l]*dum;
                        }
        }
        for (l=n-1;l>=0;l--) {
                if (indxr[l] != indxc[l])
                        for (k=0;k<n;k++)
```

```
46                                      SWAP(a[k][indxr[l]],a[k][indxc[l]]);
47              }
48      }
49      void comgaussj(MatComplex_IO &a)
50      {
51              MatComplex_IO b(a.nrows(),0);
52              comgaussj(a,b);
```

C. Sample Input File

Input file must be named infile.txt and be in the same folder as the equivalent code. The infile shown below was used to generate the data shown in Fig (5-5). On my computer (intel i7 x980) completing this run takes 50 seconds.

```
Number of Cavities: 23
Start frequency: 9150
Stop frequency: 9450
Number of points: 60000

Drive voltage:
0       0       0       0       0       0       0       0       0       0
0       0       100     0       0       0       0       0       0       0
0       0       0

Cavity Q Values:
10000   10000   10000   10000   10000   10000   10000   10000   10000   10000
10000   10000   10000   10000   10000   10000   10000   10000   10000   10000
10000   10000   10000

Frequency Values:
9307.190 9268.058 9313.955 9268.058 9313.955 9268.058 9313.955 9268.058 9313.955 9268.058
9313.955 9268.058 9313.955 9268.058 9313.955 9268.058 9313.955 9268.058 9313.955 9268.058
9313.955 9268.058 9307.190

Nearest Neighbor Coupling (1 less than # of Cavities):
0.01065 0.01065 0.01065 0.01065 0.01065 0.01065 0.01065 0.01065 0.01065 0.01065
0.01065 0.01065 0.01065 0.01065 0.01065 0.01065 0.01065 0.01065 0.01065 0.01065
0.01065 0.01065

Next Nearest Neighbor Coupling(2 less than # of Cavities):
.00145  -0.0035 .00145  -0.0035 .00145  -0.0035 .00145  -0.0035 .00145  -0.0035
.00145  -0.0035 .00145  -0.0035 .00145  -0.0035 .00145  -0.0035 .00145  -0.0035
.00145

Next Next Nearest Neighbor Coupling(3 less than # of Cavities):
0.0     0.0     0.0     0.0     0.0     0.0     0.0     0.0     0.0     0.0
0.0     0.0     0.0     0.0     0.0     0.0     0.0     0.0     0.0     0.0

Cavity response to be plotted: 13

Coupling (inductive = 1 or capacitive = 2): 2

Debug output (Y/N): n

Beadpull output (Y/N): y
```